Non-Invasive Approaches to Visualize the Endothelin Axis *In Vivo* Using State-of-the-Art Molecular Imaging Modalities

C. Höltke*[,1,2], A. Faust[1,2], H-J. Breyholz[1], K. Kopka[1,3], O. Schober[1], B. Riemann[1], C. Bremer[2,3,4], M. Schäfers[3,5] and S. Wagner[1]

[1]*Department of Nuclear Medicine, Albert-Schweitzer-Str. 33, University Hospital Münster, D-48149 Münster, Germany;* [2]*Department of Clinical Radiology, Albert-Schweitzer-Str. 33, University Hospital Münster, D-48149 Münster, Germany;* [3]*Interdisciplinary Center for Clinical Research (IZKF) Münster, Domagkstr. 3, University of Münster, D-48149 Münster, Germany;* [4]*Department of Radiology, St. Franziskus Hospital Münster, D-48145 Münster, Germany;* [5]*European Institute, Münster, Germany*

Abstract: The endothelin (ET) axis plays a major role in cardiovascular diseases and a number of human cancers. This review summarizes the work that has been published in the past ten years using labeled endothelin receptor ligands for the visualization of endothelin receptor expression *in vivo*.

Keywords: Molecular imaging, endothelin axis, tumor angiogenesis, endothelial dysfunction, cardiovascular diseases.

INTRODUCTION

The field of molecular imaging is a relatively young discipline in diagnostic medicine, which uses techniques of established methods, such as magnetic resonance imaging (MRI) [1], single photon emission computed tomography (SPECT) and positron emission tomography (PET) [2], together with newly developing technologies, such as the optical imaging procedures fluorescence reflectance imaging (FRI) and fluorescence mediated tomography (FMT) [3], in order to visualize key biological processes *in vivo*. All these techniques are in development and all exhibit assets and drawbacks. One thing they all have in common is the need for the appropriate "contrast agent". In case of scintigraphic methods the use of radiopharmaceuticals is essential, MRI, especially functional MRI (fMRI), utilizes gadolinium-chelates or iron oxide contrast agents to enhance contrast to noise ratios (CNRs) and optical imaging techniques apply fluorescent probes adressing the process under investigation.

THE ENDOTHELIN AXIS

In 1985 Kristine Hickey and her colleagues published the discovery and characterization of a vasoactive polypeptide produced by cultured endothelial cells of bovine origin [4]. The peptide was found to have potent vasoconstricting properties and its action on bovine, porcine and canine coronary artery preparations was highly dependent on extracellular Ca^{2+}-levels. Three years later, in 1988, Yanagisawa *et al.* described the structure and the special activation process of the peptide and named it endothelin [5].

Three isoforms of the 21 amino acid protein exist (ET-1, ET-2 and ET-3), which are characterized by a single α-helix and two intramolecular disulfide bridges (Fig. **1**). ET-1 excretion is regulated intracellularly by ET-1 genes which encode the mRNA for the 212 amino acid precursor protein prepro-ET-1. Several growth factors and cytokines trigger the biosynthesis of prepro-ET-1, e.g. angiotensin II, interleukin-1 and -2, vasopressin, transforming growth factor β (TGF-β), tumor necrosis factor α (TNF-α) and lipoproteins such as oxidized low-density lipoprotein (oxLDL) and high-density lipoprotein (HDL). Additionally, extrinsic factors including shear stress, hypoxia or ischemia may contribute to an increased prepro-ET-1 production. Prepro-ET-1 is then cleaved by a furin-like enzyme to yield big-ET-1, a 38-amino acid peptide, which in turn is processed by endothelin-converting-enzyme-1 (ECE-1), producing mature ET-1 (Fig. **2**) [6-8]. Antagonizing effects are found with nitric oxide (NO), prostacyclines or atrial natriuretic peptide (ANP), all interfering via second messengers cGMP or cAMP. Endothelins mediate their effects by activation of two different G-protein coupled receptor subtypes (ET_AR and ET_BR).

While ET_ARs are primarily located on vascular smooth muscle cells and are responsible for vasoconstriction and cell proliferation, ET_BRs are located on smooth muscle cells and vascular endothelial cells, causing vasodilation by the release of nitric oxide and prostacyclin and are responsible for the clearance of ET-1 from plasma in lung tissue [9]. The affinities of ET-1 and ET-2 to ET_AR are about a hundred fold higher than the affinity of ET-3. The affinity to ET_BR, however, is equal for all three isoforms [6-8, 10, 11].

This system of the three endothelin peptides and the two endothelin receptors is referred to as the endothelin axis [12]. While the concentrations of ET-1 and ET-3 in human plasma is relatively low in the healthy organism (pg/ml) and ET-2

*Address correspondence to this author at the Department of Nuclear Medicine, Albert-Schweitzer-Str. 33, University Hospital Münster, 48149 Münster, Germany; Tel.: +49-251-8347362; Fax: +49-251-8347363; E-mail: carsten.hoeltke@uni-muenster.de;
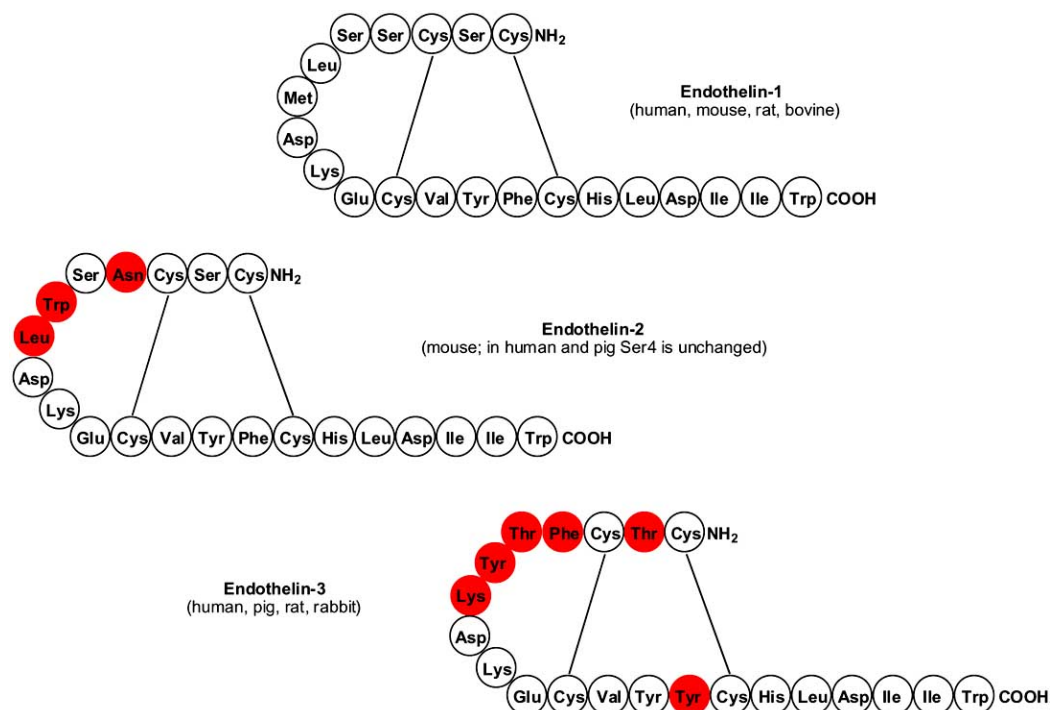
Fig. (1). The structures of the three isopeptides ET-1, -2 and -3. The modified residues in ET-2 and ET-3 are highlighted in grey color. Only in mouse ET-2 Ser4 is replaced by Asn4.
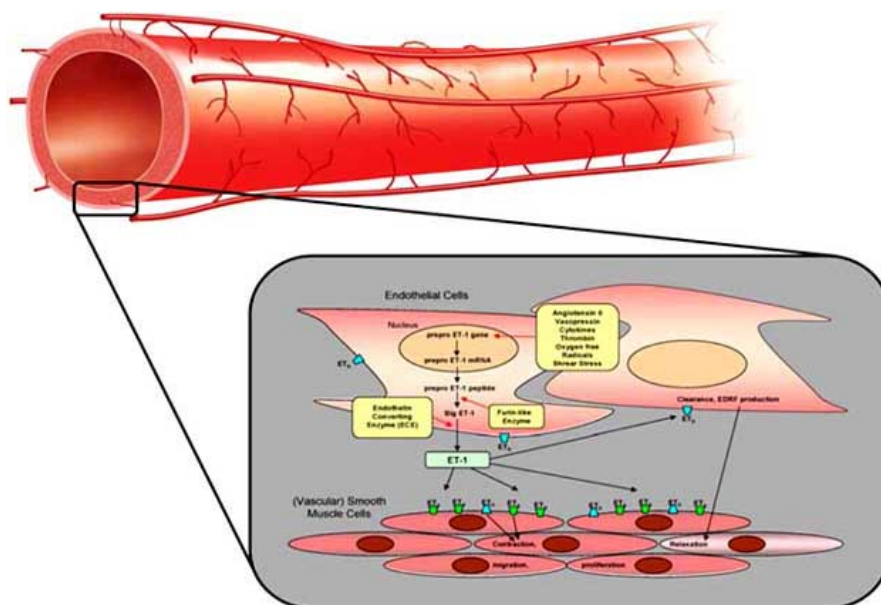

Fig. (2). Biosynthesis pathway of endothelin-1. Several trigger signals are capable of stimulating ET-1 synthesis (angiotensin II, vasopressin, thrombin etc.), starting with activation of the prepro-ET-1 gene. The prepro-ET-1 peptide is cleaved by a furin-like enzyme to yield big-ET-1 intermediates. These in turn are processed by endothelin-converting-enzyme (ECE), producing mature ET-1. The peptides interact with the two G-protein coupled receptors ET_AR and ET_BR, of which ET_AR is located primarily on (vascular) smooth muscle cells and is selective for ET-1. Activation of this receptor subtype induces vessel contraction, cell migration and tissue proliferation. ET_BR is found on both endothelial cells and (vascular) smooth muscle cells causing vessel relaxation by the release of nitric oxide and prostacyclin. In addition, ET_BRs are responsible for the clearance of ET peptides in lung tissue.

concentrations are below detection, plasma levels of ET-1 are elevated in many cardiovascular diseases. Consequently, ET receptor antagonists are used in the treatment of these diseases, and a number of different peptidic and non peptidic ligands, both selective and unselective, have been developed to improve efficacy [13-17].

But not only its influence on the cardiovascular system arouses interest in the endothelin system, it also plays an

important role in the pathophysiology of certain human cancer types [12, 18-20]. Recent data suggest that endothelins, especially ET-1, are highly relevant for the progression of a variety of tumor types including prostatic [21], breast [22, 23] and ovarian carcinoma [24, 25], Karposi's sarcoma, [26] melanoma [27] and lung malignancies [28, 29]. Endothelins play a role as paracrine as well as autocrine factors, promoting tumor growth by inducing cell proliferation and angiogenesis and by inhibiting apoptosis. ET-1 acts by activating downstream signaling pathways, starting with the activation of phospholipase C (PLC) which acts on calcium metabolism and activates protein kinase C (PKC). PKC regulates the mitogenic activity of surrounding cells (by activating mitogen activated protein kinase MAPK), affects the apoptotic pathway (by exerting influence on phosphorylation pathways) and promotes neovascularisation (by amplifiying the transcription of growth-related genes or increasing vascular endothelial growth factor VEGF production) [30, 31].

In addition, the endothelin axis participates in diabetes [32, 33], arthritis [34], chronic kidney diseases [35] and is discussed as a relevant factor in fibrotic diseases such as systemic sclerosis [36]. In summary, whenever the endothelin axis is dysregulated, severe diseases may develop. Consequently, it is easy to understand why many scientific research groups have become interested in imaging approaches to visualize the endothelin axis *in vivo*.

PEPTIDIC LIGANDS

The first radioligands targeting endothelin receptors were the iodine-125-labeled peptide [^{125}I]ET-1 [37, 38], the ET_BR selective [^{125}I]BQ3020 [39, 40] and the short linear peptide [^{125}I]PD 151242 [41, 42], but these have not been discussed for *in vivo* imaging applications. However, since these peptides were long and extensively used as ligands for studying endothelin receptors *in vitro* and *ex vivo*, it is perspicuous that labeling endothelin derived peptides with radionuclides suitable for *in vivo* imaging techniques was the method of choice. Short peptides possessing the Leu-Asp-Ile-Ile-Trp amino acid sequence of mammalian endothelin peptides at the C-terminus and different amino acid residues at the N-terminus were found to be highly affine to endothelin receptors [43, 44]. First attempts for *in vivo* imaging of endothelin receptors in atherosclerotic plaques were made by labeling a so derived short peptide with the most prominent γ-emitting nuclide for SPECT and planar scintigraphy technetium-99m (^{99m}Tc). The peptide used, Asp-Gly-Gly-Cys-Gly-Cys-Phe-(D-Trp)-Leu-Asp-ile-Ile-Trp, is an endothelin derivative with an N-terminus capable of chelating a metal (Fig. **3A**) and an affinity to the ET_A receptor of 370 nM [45, 46]. Johannsen and colleagues [47] found that reaction of the peptide with a [^{99}Tc]-gluconate precursor resulted in the formation of two separable metal complexes with presumably contrarily oriented peptide side chains and 1:2 stochiometry (Fig. **3B,C**). Analogously labeling the peptide with ^{99m}Tc was achieved with > 95% radiochemical yield. The labeled peptide was then used in a model of experimental atherosclerosis in New Zealand White rabbits [48]. Animals underwent balloon denudation of the right iliac artery and the infrarenal aorta and were fed a high cholesterol diet for six weeks to induce plaque formation. Fifteen minutes after intraveneous administration of 74 MBq of the labeled peptide planar scintigraphy revealed a high accumulation of radioactivity in heart, liver, lung and kidneys. In addition, a rapid renal excretion was confirmed by a high amount of radioactivity in the bladder. The lesions induced in the infrarenal aorta could clearly be visualized (Fig. **4**), consistent with the pathological expression of endothelin receptors on proliferated neoin-
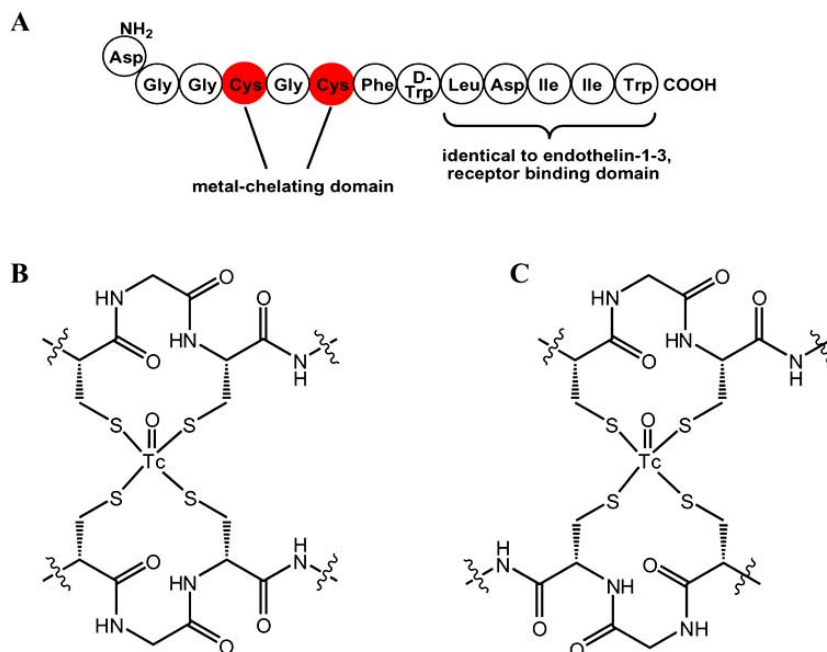

Fig. (3). A) Structure of the first synthetic peptidic ligand targeting the endothelin receptors. The cystein residues Csy4 and Cys6 chelate the metal ion, the residues Leu9 to Trp13 are identical to the C-terminus of endothelins 1-3 of mammalian origin and are responsible for receptor binding. B) + C) Proposed chelate arrangements of the two cysteinyl residues around the metal center with parallel (B) and anti-parallel (C) orientation of the peptide chain [45, 47].
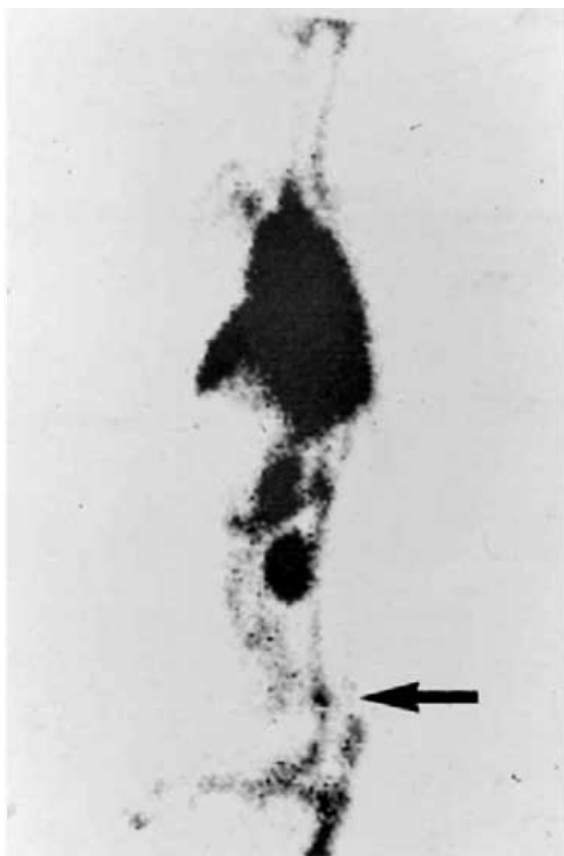
Fig. (4). Left lateral scintigram of a rabbit after balloon denudation of the right iliac artery and the infrarenal aorta and after six weeks of a high cholesterol diet. The neointimal lesions located in the infrarenal aorta (arrow) were imaged *in vivo* 15 min after injection. Accumulation of the Tc-99m-endothelin derivative is also apparent in the heart, liver and kidneys (reprinted with permission from *Elsevier B.V.* [48]).

timal smooth muscle cells. A correlation to the amount of macrophages or the size of the lesion, however, was not possible.

In contrast to ^{125}I, the iodine isotope ^{123}I possesses a higher decay γ-energy (159 keV vs. 27 - 35 keV) that is suitable for *in vivo* SPECT imaging. Just like the heavier isotope ^{123}I can be provided as the anion in saline or alkali solution and thus can be introduced into tyrosine residues of peptides and proteins by electrophilic aromatic addition. Gibson *et al.* labeled ET-1 with ^{123}I using this method (Fig. **5A**). They measured the biodistribution of [^{123}I]ET-1 in comparison to the ^{125}I-labeled isotopomer [^{125}I]ET-1 in rat and rhesus monkey by planar scintigraphy and found a high accumulation of the tracer in lung, liver and kidneys [49]. The application of a non-specific endothelin receptor antagonist (L-749329 [50]) prior to radiotracer administration caused a dose-dependent decrease in tracer uptake in lung and liver. In contrast to *ex vivo* examinations with [^{125}I]ET-1 a decrease in kidney uptake was not observed *in vivo* using [^{123}I]ET-1 and L-749329.

The positron emitting nuclide ^{18}F is widely used for labeling small molecules and peptides for *in vivo* imaging approaches using PET. Johnstrøm *et al.* used a variation of the Bolton-Hunter reagent [51], *N*-succinimidyl-4-[^{18}F]fluoro-benzoate ([^{18}F]SFB, Fig. **5D**) for the labeling of the endothelin-B-receptor selective peptidic agonist BQ3020 [52, 53]. BQ3020 is an acetyl-protected, truncated ET-1 derivative devoid of an N-terminal pentapeptide and the two cystein residues Cys11 and Cys15, which are replaced by alanine (acetyl-(ala^{11,15})-endothelin-1$_{(6-21)}$). The ^{125}I-labeled derivative of this peptide is prevalently used for *in vitro* and *ex vivo* studies analogously to [^{125}I]ET-1 [40, 54]. The active ester [^{18}F]SFB reacts with the amino group of Lys4 of BQ3020, yielding the radiolabeled peptide (Fig. **5B**) in about 3% total radiochemical yield after a 4 hour synthesis. *In vitro* characterization of the tracer using human lung, kidney and heart confirmed a single subnanomolar affinity and ET_B selectivity. Visualization of tracer binding was possible by autoradiography with normal and diseased human tissue, revealing a high level of binding to ET_B receptors in lung and kidney medulla, whereas kidney cortex and heart showed lower levels of ET_B receptor expression. Additionally, in atherosclerotic coronary arteries, high levels of ET_B receptor densities were found to colocalize with macrophages. *In vivo* biodistribution experiments were carried out in New Zealand White rabbits with a microPET P4 imaging system. High levels of [^{18}F]BQ3020 binding were found in lung, liver, and kidney. In the kidneys, a heterogeneous distribution of radioactivity was observed, confirming the results from the autoradiographical examinations. The ET_A-rich myocardium could not be visualized with this tracer, as expected for an ET_B selective substance [55].

In a similar manner the radiolabeling of ET-1 itself was realized by Johnstrøm *et al.* [56]. Radiochemical purities of the labeled product [^{18}F]ET-1 were > 95% with a specific activity of 220-370 GBq/μmol. The obtained radiochemical yield was 6% after a total synthesis and purification time of 3½ hours. Dynamic PET data of [^{18}F]ET-1 in male Sprague-Dawley rats demonstrated that the radioligand rapidly accumulated in the lung, kidney, and liver which is consistent with receptor localization. However, the visualized receptor density in the heart was unexpectedly low compared to that predicted from *in vitro* investigations. The tracer binding in lungs could not be displaced by the ET_BR selective antagonist BQ788 in agreement with a proposed rapid internalization of ET-1 (and [^{18}F]ET-1) by ET_BRs. In contrast, predosing with BQ788 significantly reduced the amount of [^{18}F]ET-1 in the ET_BR-rich lung and kidneys, and the ET_AR-rich heart could be visualized by small animal PET studies. In summary, the data suggest that [^{18}F]ET-1 uptake by ET_BRs in the lung and kidneys reduces the amount of tracer available for binding to receptors of the heart in the chosen animal model [57].

NON-PEPTIDIC LIGANDS

Due to their rapid metabolism in the gastrointestinal tract and their short duration of action the clinical use of peptidic antagonists is quite limited. Thus, in addition to the mentioned peptidic endothelin receptor ligands a number of non-peptidic receptor antagonists, both selective and non-selective, have been developed [58]. The large majority of these compounds is ET_AR selective; only a few reports about non-peptidic antagonists with ET_BR selectivity have been
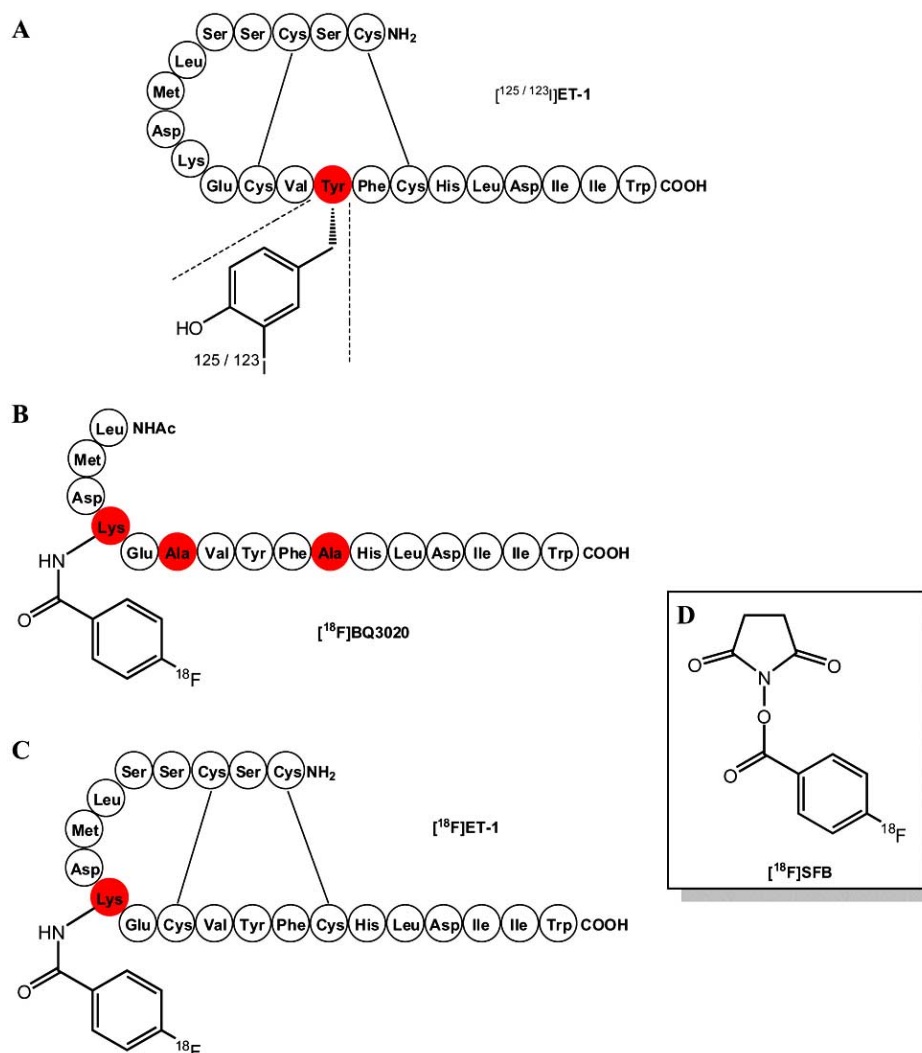
Fig. (5). Structures and labeling sites of the peptidic ligands [^{125}I]ET-1 and [^{123}I]ET-1 (A), the ET$_B$R selective compound [^{18}F]BQ3020 (B) and [^{18}F]ET-1 (C). Grey residues indicate the sites of modification. Radioactive iodine is introduced by electrophilic substitution of the phenol function of Tyr13 using [^{123}I]NaI or [^{125}I]NaI and chloroamine-T as oxidant (A). BQ3020 (B) lacks the cystin bridges and an N-terminal pentapeptide, Cys11 and Cys15 are replaced by alanine. For introducing the PET radionuclide fluorine-18 the Bolton-Hunter-type reagent *N*-succinimidyl-4-[^{18}F]fluorobenzoate, [^{18}F]SFB (D) has been used, which selectively forms an amide bond with the ε-amino group of Lys4 of BQ3020 (B) or Lys9 of ET-derived peptides (C).

published [59, 60]. The main drawback for the clinical use of these drugs is their liver-toxicity, which probably is caused by an impaired bile excretion [61-63]. Fig. (6) shows a number of structures of endothelin receptor antagonists. Three of these, Bosentan [64], Enrasentan [65] and Tezosentan [66] are mixed endothelin receptor ligands with a less than 100-fold selectivity for ET$_A$R. Edonentan, on the other hand, has an ET$_A$R selectivity of > 80.000-fold vs. ET$_B$R and, in addition, is extremely potent with a K_i-value of 10 pM for ET$_A$R [67].

The first non-peptidic ligand to be modified for imaging purposes was PD 156707. This compound belongs to the group of butenolide antagonists that were extracted out of a > 150.000 compound library at *Parke-Davis Pharmaceutical Research Laboratories* and displayed competitive antagonism with IC$_{50}$ values of 0.31 nM and 420 nM for the ET$_A$ and ET$_B$ receptor, respectively [68, 69]. A modification of

the trimethoxyaryl moiety with a short spacer and a phenoxy group permitted radiolabeling with [^{125}I]-iodide, which was accomplished by a collaboration of *Amersham International plc* (now part of *GE Healthcare*) and the *Clinical Pharmacology Unit* at the *University of Cambridge School of Clinical Medicine*, resulting in the dedicated radiopharmaceutical [^{125}I]PD 164333 (Fig. **7A**) [70]. *In vitro* saturation binding assays revealed that the radioligand bound with high affinity to a single population of receptors in human aorta, left ventricular myocardium and kidney. Kinetic experiments showed that binding was reversible and competition binding assays with unlabeled PD 164333 and [^{125}I]ET-1 indicated a retained affinity and selectivity for ET$_A$R. In healthy human tissue, autoradiography examinations provided evidence that the tracer predominantly bound to vascular structures in brain, kidney, myocardium and lung. In coronary arteries containing advanced atherosclerotic lesions, [^{125}I]PD 164333 binding was mainly localized to the medial layer, with little
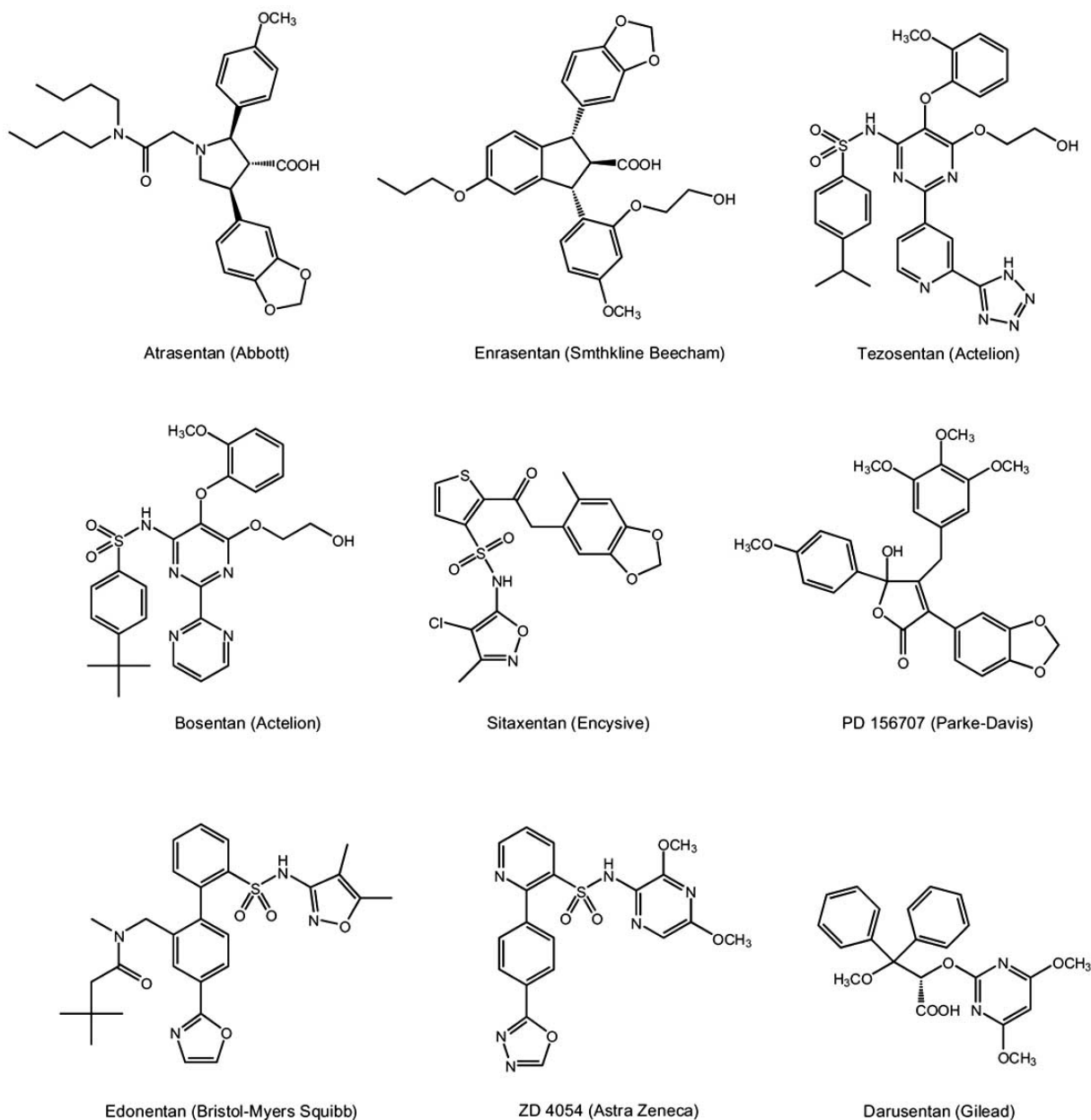
Fig. (6). Structures of typical (selective and non-selective) endothelin receptor antagonists (neutral forms), which have been or are currently evaluated in clinical trials. Recurring motifs are a multiaromatic backbone and either a (hetero)aromatic sulfonamide or a carboxylic acid. Bosentan, Enrasentan and Tezosentan are orally available mixed ET_AR/ET_BR antagonists. Bosentan is already approved for use in pulmonary arterial hypertension (PAH) patients in the United States and the European Union. Sitaxentan has been approved for PAH patients in the European Union, in Canada and in Australia but not yet in the United States. Atrasentan is a bioavailable receptor antagonist with long lasting action and has been investigated for the treatment of hormone-refractory prostate cancer.

tracer binding to the intimal layer (Fig **7B**). Similarly, in saphenous veins used for bypass grafting, highest tracer accumulation was detected in the vascular smooth muscle cells of the medial layer with little or no activity present in the proliferated smooth muscle of the occlusive lesions (Fig **7C**). The obtained results propelled the possibility of using this tracer for *in vitro* and *in vivo* imaging experiments into the center of interest. Two years later, in 2000, the same group published the synthesis of the first non-peptidic endothelin receptor radioligand for PET based on the PD 156707 lead structure. They realized the radiolabeling with the positron emitting nuclide carbon-11 via ^{11}C-methylation of the phenoxy precursor derivative PD 169390 using [^{11}C]methyl iodide, resulting in [^{11}C]PD 156707, the authentically radiolabeled isotopomer (Fig. **8**) [52]. However, the use of this compound for *in vivo* imaging has not been described, maybe due to the relatively low specific activity of the preparation (< 20 GBq/μmol) which may not be suitable for endothelin receptor imaging.

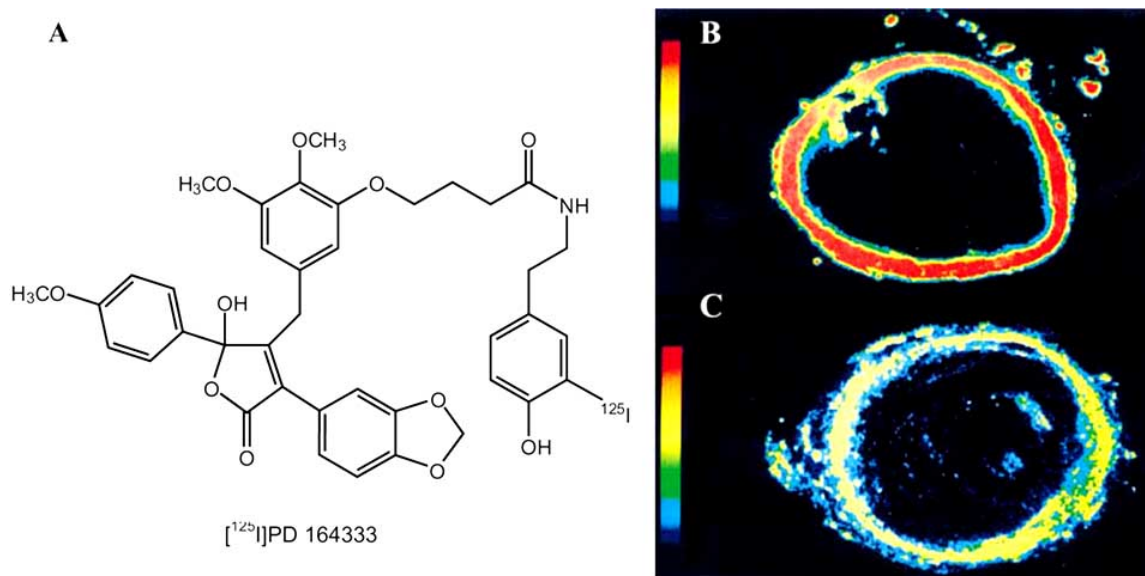In the same year the group of Robert F. Dannals at *Johns Hopkins Medical Institution* in cooperation with *Merck Re-*

Fig. (7). A) Structure of [^{125}I]PD 164333, synthesized by Davenport *et al.* as the first non-peptidic endothelin receptor antagonist for molecular imaging purposes. *In vitro* evaluation of this tracer revealed high affinity and selectivity for ET$_A$R. B) Autoradiography on human coronary arteries containing advanced atherosclerotic lesions, tracer binding was mainly found on the medial layer, with little tracer binding to the intimal layer. C) In saphenous veins used for bypass grafting, highest tracer accumulation was detected in the vascular smooth muscle cells of the medial layer with little or no binding present on the proliferated smooth muscle of the occlusive lesion (reprinted with permission from *Macmillan Publishers Ltd.* [70]).
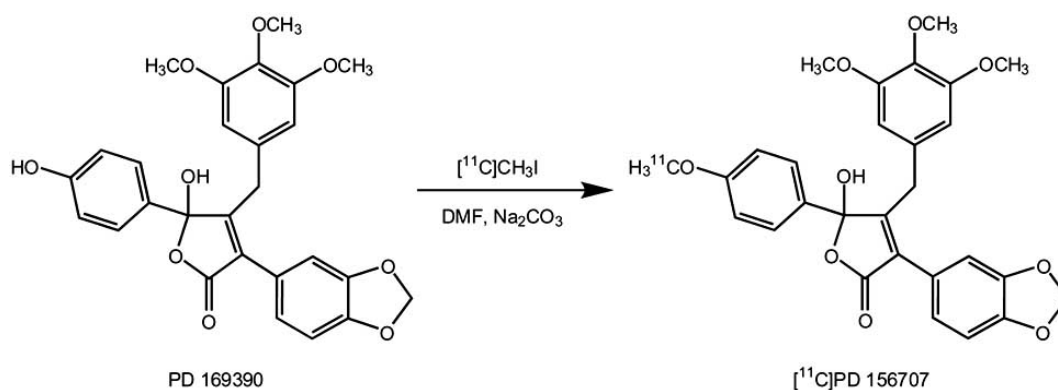

Fig. (8). Radiosynthesis of [^{11}C]PD 156707, realized by methylation of the phenoxy precursor PD 169390 with [^{11}C]CH$_3$I [52].

search Laboratories reported about the synthesis of a PET radioligand for endothelin receptors based on a lead structure related to Enrasentan, namely L 753037 (Fig. **9**) [71]. This ligand had been developed by *Banyu Pharmaceutical* and was further processed jointly by *Merck* and *Banyu*. L 753037, as Enrasentan, is a highly affine but non-selective endothelin receptor ligand with affinities of $K_i = 34$ pM (ET$_A$R) and $K_i = 104$ pM (ET$_B$R) [72]. The radiosynthetic method that was used for tracer preparation is similar to the one described above. The ^{11}C-labeled counterpart of L 753037 was synthesized by methylation of the phenoxy precursor using [^{11}C]methyl iodide under basic conditions (tetrabutylammonium hydroxide in DMF at 80°C). The radiochemical yield, however, was low ($\leq 5\%$, decay corrected) probably due to the formation of byproducts. Specific activities reached with this radiolabeling method were around 90 GBq/µmol after a short time for preparation and purification (17 minutes). Just a year later the first results of *ex vivo* dissection studies and *in vivo* imaging experiments

with this radioligand were reported [73]. *Ex vivo* biodistribution data obtained after intravenous injection of 7.4 MBq of the tracer into CD-1 mice showed that uptake in liver, kidneys and the lung was predominant ($\approx 60\%$ ID/gram) at early time points. Two hours after injection tracer accumulation in the lung still was 41% of the peak activity and uptakes in liver and kidneys were reduced to 27% and 19%, respectively. In contrast, the uptake in the heart remained nearly constant for this period of time at $\approx 5.6\%$ ID/gram. Dynamic *in vivo* PET experiments were conducted in a male beagle dog. The results show a high accumulation of the tracer in the wall of the dog heart at 55–95 min after injection (Fig. **9 A**) and a significant reduction in binding (P < 0.001) after administration of the selective ET$_A$R inhibitor L 753164 (1.0 mg/kg; Fig. **9B**).

In 2001 the radiosynthesis of an ^{18}F-labeled analogue of the moderately ET$_A$R-selective (≈ 90:1) antagonist SB 209670 was reported. Peter Johnstrøm and Anthony P. Dav-
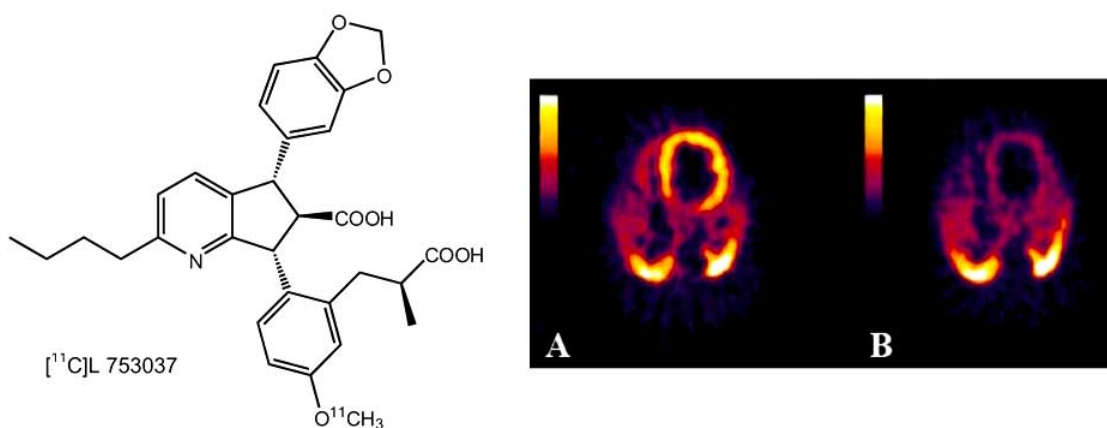
Fig. (9). Structure of [^{11}C]L 753037, an unselective endothelin receptor antagonist. The first *in vivo* PET imaging experiments with this radiotracer were conducted in a male beagle dog. The results show high accumulation of [^{11}C]L 753037 in the wall of the heart at 55–95 min after injection (Fig. **9A**) and a significant reduction in binding (P < 0.001) after administration of the selective ET$_A$R inhibitor L 753164 (Fig. **9B**, reprinted with permission from *The Journal of Nuclear Medicine* [73]).

enport from *Cambridge* presented a three step radiolabeling procedure [74]. In the first step the radiolabeling synthon [^{18}F]fluoropropylbromide was generated by nucleophilic substitution reaction of [^{18}F]fluoride and 1,3-dibromopropane. In the second step the radiolabeling of the phenoxy precursor was performed. The third step removed the ester protective groups (Fig. **10**). The overall radiochemical yield for this sophisticated reaction procedure was 15% (decay corrected), the radiochemical purity of the isolated ligand was 99% and the specific activity of the preparation was 100 - 150 GBq/μmol. Three years later the *in vitro* and *in vivo* evaluation of this radiotracer was described [75]. *In vitro* experiments with sections of human tissue indicated that [^{18}F]SB 209670 binds predominantly to ET$_A$Rs in the human heart and kidney. Dynamic PET data was collected from two experiments with Sprague-Dawley rats using a microPET P4 scanner. The highest tracer uptake was found in the liver,

where radioactivity counts peaked at early time points (2.5 min) and a subsequent increase of counts in regions inferior to the liver, indicating a high degree of liver and bile metabolism and excretion via the small intestine. However, a detectable tracer uptake in the heart wall of the animal was also delineated (Fig. **11**), suggesting a binding of the ligand to myocardial ET$_A$Rs.

Another radioligand based on the already mentioned lead structure of PD 156707 was introduced in 2006. Our group was able to radioiodinate the phenoxy precursor compound PD 169390 with [^{123}I]iodide and [^{125}I]iodide in the presence of chloroamine-T in excellent radiochemical yields (70% - 90%) and high specific activities (8.6 TBq/μmol for the ^{123}I derivative) [76]. SPECT imaging with the ^{123}I derivative was possible but despite the good *in vitro* affinity of the non-radioactive counterpart (K$_i$ = 1.0 nM towards ET$_A$R, selectivity ≈ 1300:1) to murine myocardial membranes an *in vivo*
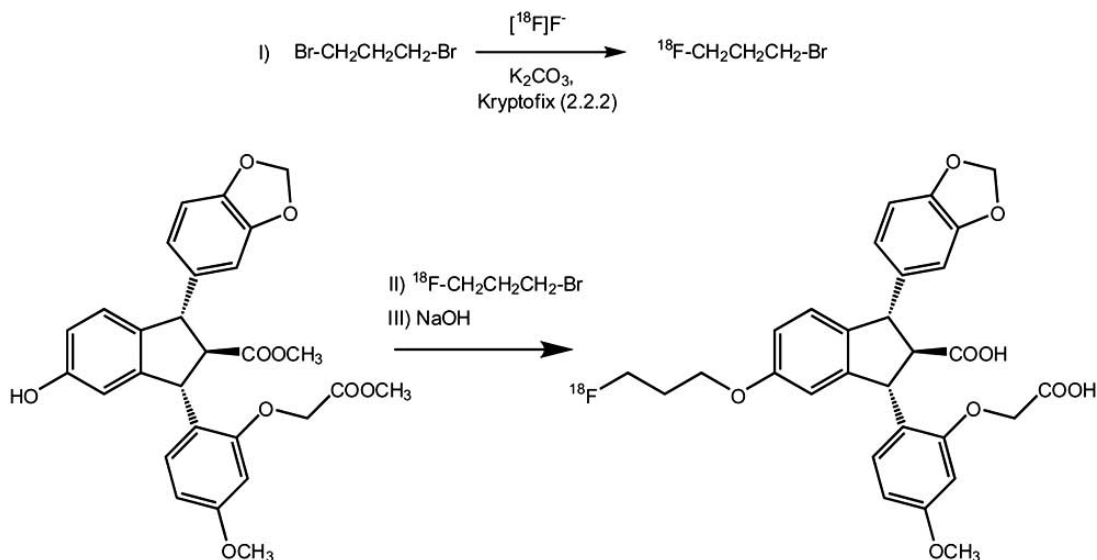

Fig. (10). Scheme of the three step radiolabeling procedure developed by Johnstrøm *et al.* for the synthesis of [^{18}F]SB 209670. The first step requires the synthesis of [^{18}F]fluoropropylbromide. This radiolabeling synthon is separately purified and reconstituted. The next step is the labeling of the phenoxy precursor compound with the radiolabeling synthon, followed by a final deprotection of the ester protective groups [75].
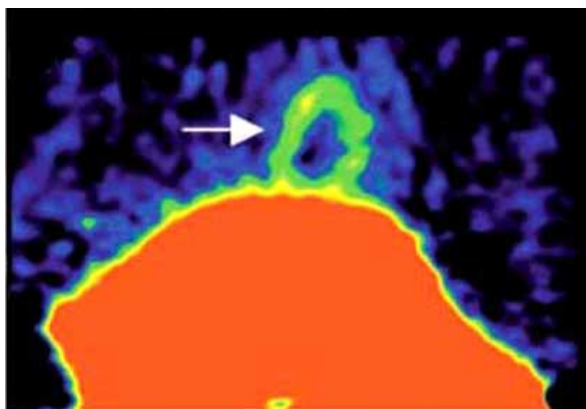
Fig. (11). Coronal image of a rat after administration of 51 MBq of [^{18}F]SB 209670 (average data 31 - 120 minutes). The heart wall is clearly visible (white arrow), together with a high signal intensity in liver and intestine (reprinted with permission from *Lippincott Williams & Wilkins* [75]).

binding to endothelin receptors in mice could not be confirmed. Also, biodistribution studies in wild-type mice were not able to define specific binding.
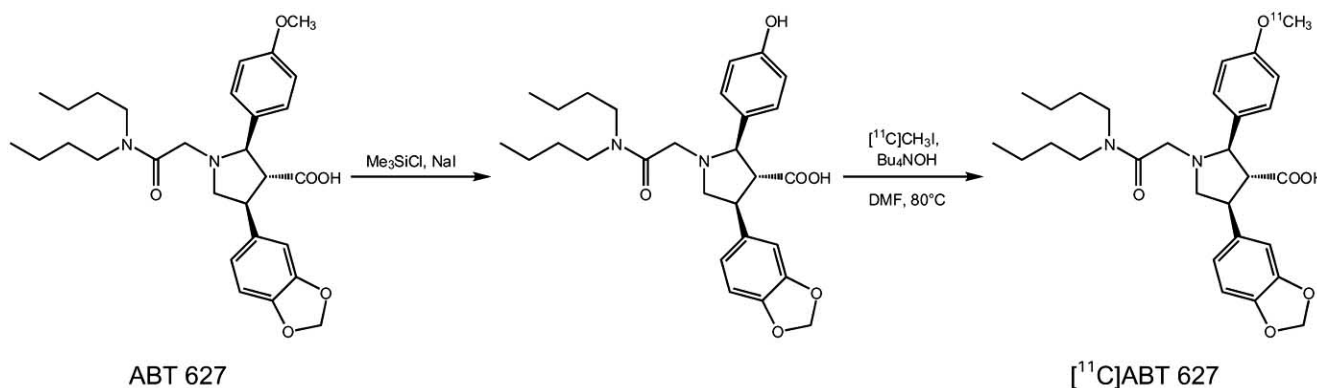
The highly selective ET$_A$R antagonist Atrasentan [77] (ABT 627) was selected as a lead structure for ^{11}C-labeling by the *Johns Hopkins* group in cooperation with *Abbott Laboratories* in 2006 [78]. They used the drug itself – supplied by *Abbott* – as the starting material for their synthetic approach (Fig. **12**). A desmethylation reaction was applied to provide the phenoxy precursor compound, which in turn was re-methylated with [^{11}C]methyl iodide by the same method as described above for L 753037. After an average time for radiosynthesis, HPLC purification and formulation of only 26 min they obtained the tracer, [^{11}C]ABT 627, in a radiochemical yield of 14% based on [^{11}C]methyl iodide. The average specific activity was 245.2 GBq/μmol at the end of synthesis with a radiochemical purity of > 96%. The synthesized radiotracer was evaluated by *ex vivo* biodistribution studies in CD-1 mice. [^{11}C]ABT 627 showed highest uptake in the liver, kidneys and lungs. No significant binding was observed in mouse brain or heart, suggesting a rapid metabolism of the tracer *in vivo*. However, PET imaging experiments in a baboon were able to confirm specific binding of the radiotracer in heart and lung tissue. Time–activity curves (Fig. **13**) derived from these studies showed an about 50% reduction in signal intensity after preinjection of 0.39 mg/kg of unlabeled Atrasentan for the myocardium and the lung at

Fig. (12). Synthetic route for [^{11}C]Atrasentan ([^{11}C]ABT 627). The desmethylation of ABT 627 with trimethylsilyl iodide, generated *in situ* from trimethylsilyl chloride and sodium iodide, yields the phenoxy precursor compound, which in turn was re-methylated by reaction with [^{11}C]methyl iodide in DMF using tetrabutylammonium hydroxide as base [78].
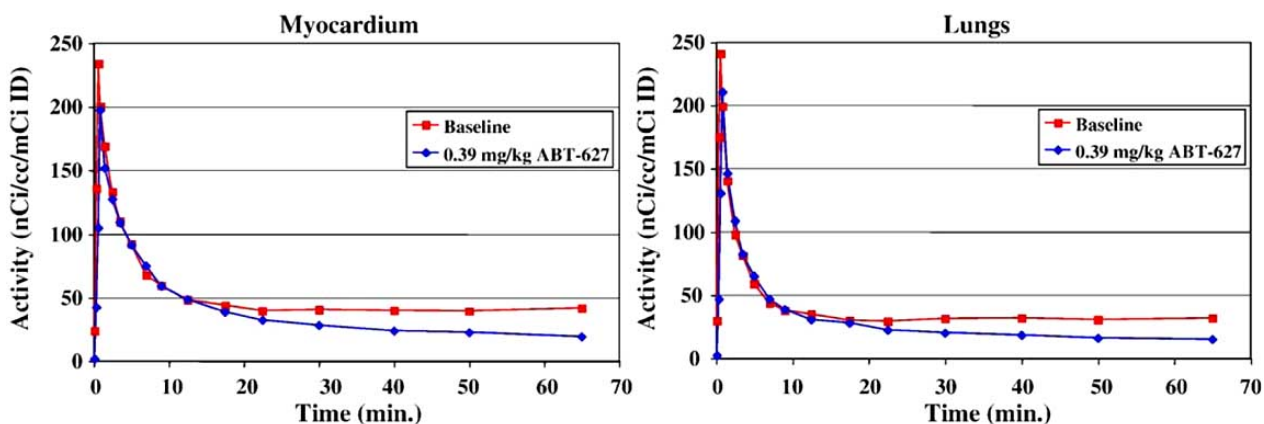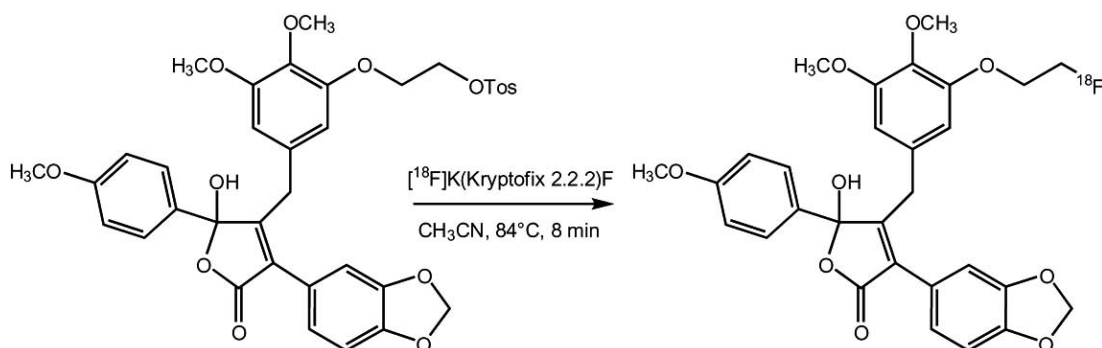

Fig. (13). Time-activity-curves of the myocardium and the lungs generated by *in vivo* PET imaging studies with one baboon. The red curves show baseline values after administration of ≈ 460 MBq of [^{11}C]ABT 627, the blue curve displays the values after preinjection of 0.39 mg/kg unlabeled ABT 627. After 65 minutes a reduction in tissue activity of ≈ 50% can be observed (reprinted with permission from *Elsevier B.V.* [78]).

Fig. (14). Radiofluorination of a designated tosylate precursor for [18F]fluoroethoxy-PD 156707. Substitution with [18F]fluoride was carried out with an average radiochemical yield of 22% (n = 12, decay corrected) and a radiochemical purity of 99 %. The specific activities were variable and did not exceed 60 GBq/μmol [79].

65 min p.i.. The authors concluded that the radiotracer bound to ET receptors, although they admitted that further studies were needed for confirmation.

A further approach towards an ^{18}F-fluorinated PET radio-ligand was described by our group in 2007 [79a]. The lead compound PD 156707 was modified to enable radiofluorination with the [18F]K(Kryptofix 2.2.2)F complex. For that purpose we synthesized a tosylate precursor derivative by multistep organic synthesis. Substitution with [18F]fluoride was carried out with an average radiochemical yield of 22% (n = 12, decay corrected) and a radiochemical purity of 99% (Fig. **14**). The non-radioactive reference compound was evaluated *in vitro* and displayed a high affinity and selectivity for ET_AR (K_i = 1.1 nM, selectivity vs. ET_BR = 220:1) in mouse myocardial membranes. In spite of these encouraging results the specific activities of the [18F]fluoroethoxy-PD

156707 preparations were very variable and did not exceed 60 GBq/μmol. However, a visualization of myocardial tracer uptake as evidence for receptor binding was possible, although a major hepatobiliary route of excretion together with a rapid metabolism into polar radiometabolites complicated the interpretation of imaging data [79b].

In 2008 Mathews and colleague presented a project which emerged from a cooperation with *Bristol-Myers Squibb* (BMS). Five years ago BMS had developed the very highly affine and selective ET_AR antagonist Edonentan or BMS-207940 (K_i = 10 pM, selectivity vs. ET_BR = 80000:1) [67], and they provided valuable precursor derivatives for this work. Modifications of the original antagonist yielded precursor compounds for radiolabeling with [18F]fluoride as well as [11C]methyl iodide (Fig. **15**) [80]. The radiomethylation procedure was conducted as described in earlier publica-
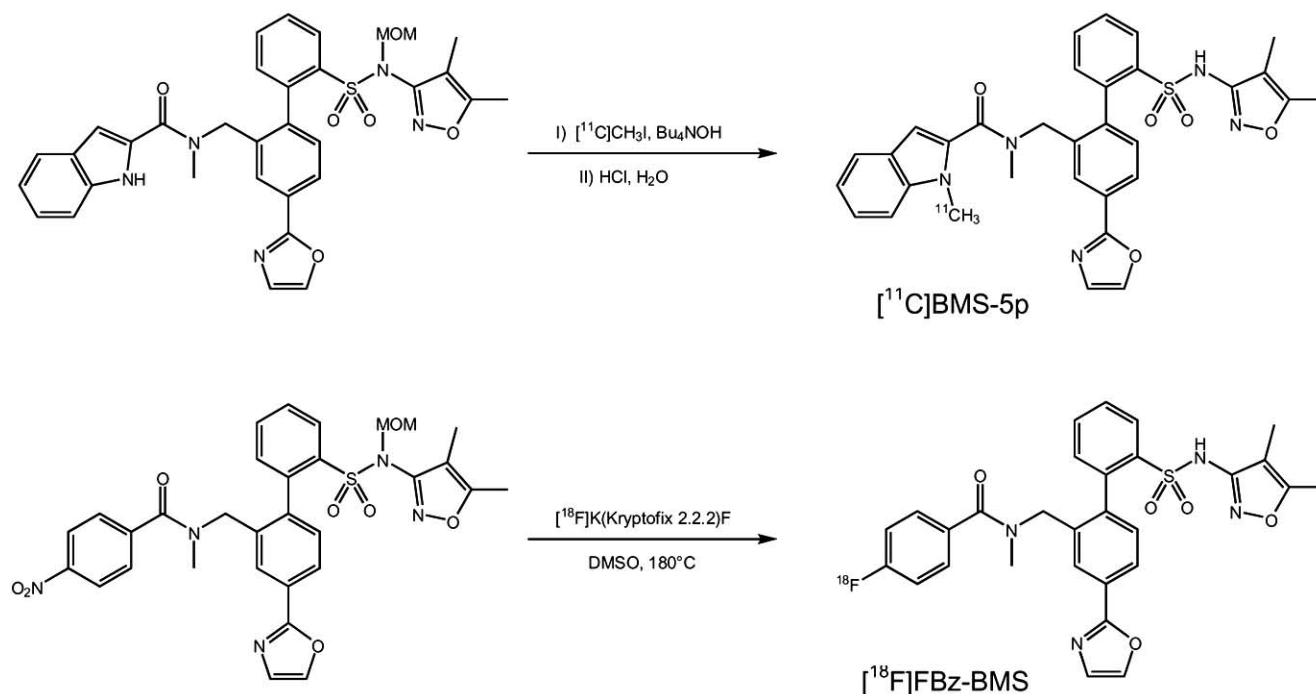

Fig. (15). Pathways to the radiolabeled BMS 207940 derivatives [11C]BMS-5p and [18F]FBz-BMS [80]. In case of the radiomethylation to [11C]BMS-5p a deprotection step was necessary to remove the methoxymethyl (MOM) ether from the sulfonamide group. The harsh reaction conditions of the radiofluorination procedure rendered a further deprotection step unnecessary.

tions, using [11C]methyl iodide and tetrabutylammonium hydroxide in DMF. Radiofluorination was accomplished by reaction of the *p*-nitroaryl precursor with the [18F]-K(Kryptofix 2.2.2)F complex in DMSO at 180°C. The methylated radioligand [11C]BMS-5p was prepared in 36 minutes with a radiochemical yield of ≈ 1.5% (uncorrected for decay) and a specific activity of only around 1.0 GBq/µmol at the end of synthesis. The low specific activity was assigned to an incomplete deprotection of the precursor after radiolabeling. [18F]FBz-BMS was obtained in 130 min with an average radiochemical yield of 0.54% (uncorrected for decay) and a specific activity of 12.9 GBq/µmol at the end of synthesis. The radiochemical purity of the radioligands was greater than 99% in both cases. Despite the low radiochemical yields enough radiotracer for biological evaluation could be produced. Biodistribution studies in mice showed that for both radioligands the highest uptake was found in liver, lungs, kidneys and heart. Radioactivity in liver and kidneys washed out over time, uptake in lungs and heart remained relatively stable. *In vivo* PET imaging in a baboon using both radioligands confirmed the utility of these compounds for delineating ET$_A$Rs. Competition studies with Edonentan (BMS 207940) at 1.0 mg/kg revealed a reduction of radioactivity in the myocardium of 85% for both

[18F]FBz-BMS and [11C]BMS-5p (Fig. **16**).

Table **1** summarizes the radiotracers which have been used for *in vivo* imaging of endothelin receptors so far. The displayed affinities and specificities are mainly extracted from different publications describing the non-labeled ligands and their pharmacological profile.

Optical imaging can be an attractive alternative to scintigraphic imaging techniques. It is relatively inexpensive, free of ionizing radiation hazards and isotope decay, and applicable for tomographic (FMT) and surface-weighted (FRI) detection methods. These techniques allow the detection of molecules in picomolar concentrations, which is comparable to conventional scintigraphic imaging techniques [3, 81-84]. As well as high signal to noise ratios (SNRs), imaging in the near infrared range (λ = 650 nm - 950 nm) shows very efficient tissue penetration as the absorption by water and hemoglobin is relatively low ('diagnostic window', Fig. **17A**). In 2007 our group presented the first endothelin receptor ligand modified for optical imaging based on the ET$_A$R selective PD 156707 lead structure [85]. A derivative of PD 156707 with a polyethylene glycol (PEG) spacer group containing an amino functionality was synthesized and labeled with a fluorescent dye without changing the ET$_A$ binding
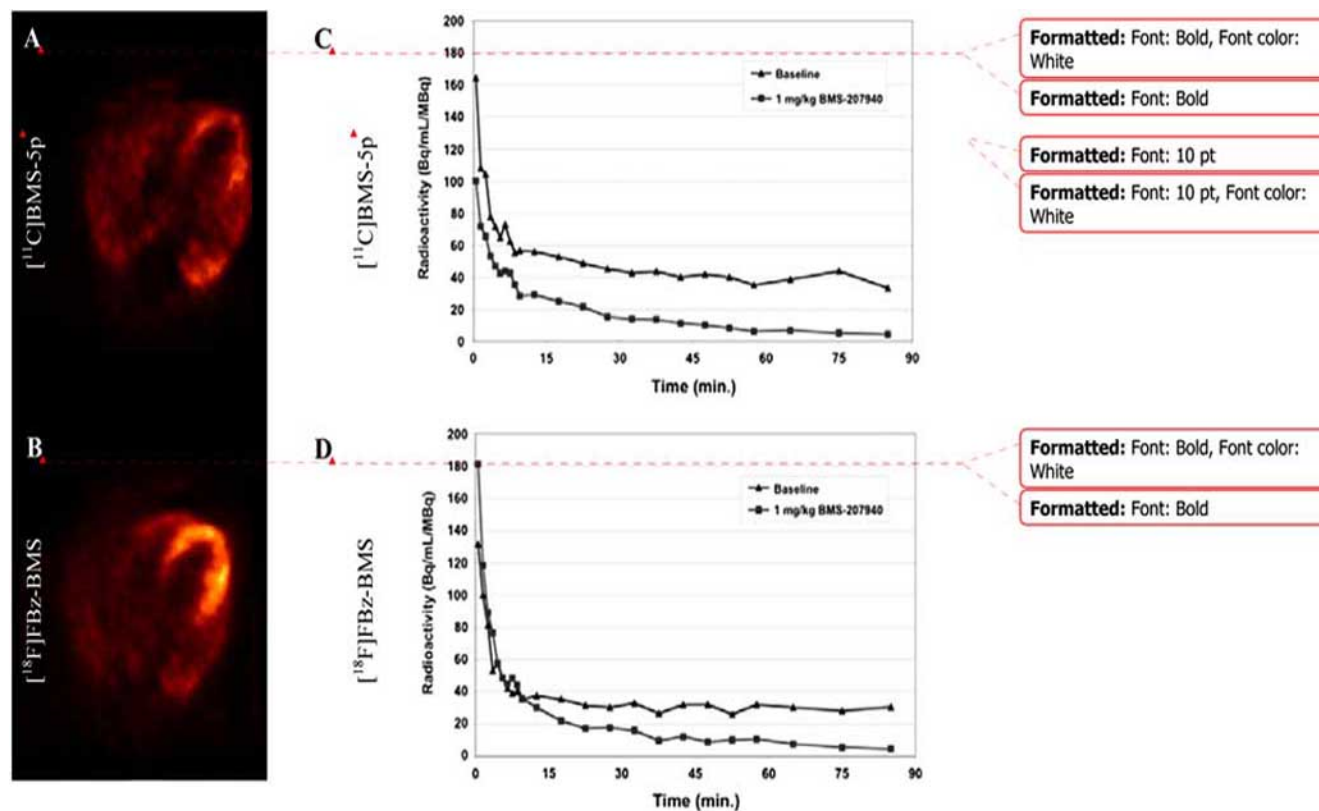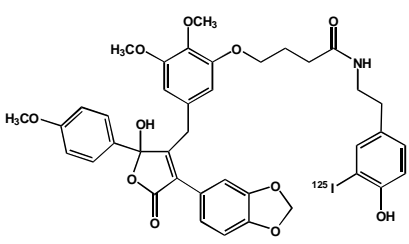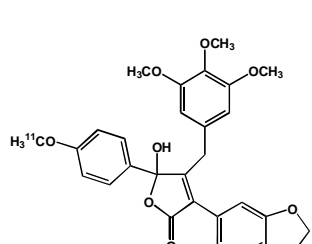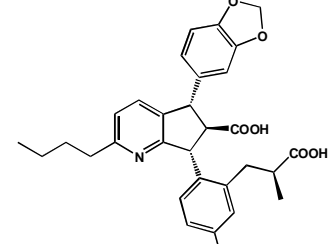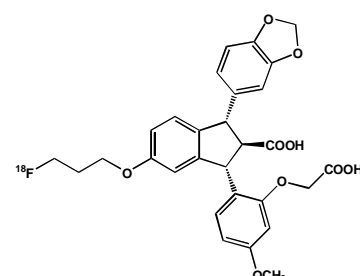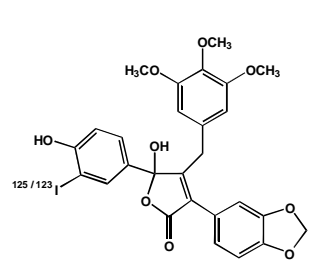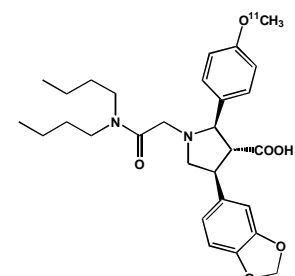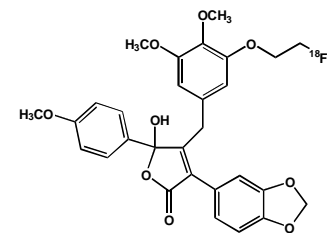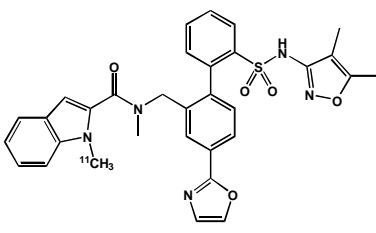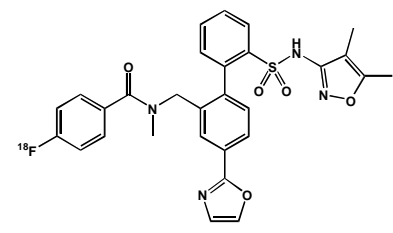

Fig. (16). PET-images of a baboon 40-90 minutes after administration of ≈ 290 MBq of [11C]BMS-5p (A) or ≈ 160 MBq of [18F]FBz-BMS (B). The wall of the left ventricle is clearly visible, together with some intensity in the lungs. Region of interest (ROI) analysis of the myocardium shows that [11C]BMS-5p reached equilibrium earlier (baseline, C) than [18F]FBz-BMS (baseline, D), but both radioligands showed 85% specific binding at 85 min after injection as shown by preinjection of 1 mg/kg of Edonentan (BMS-207940). Reprinted with permission from *The Journal of Nuclear Medicine* [80].

Table 1.   Non-Peptidic Endothelin Receptor Radioligands and Corresponding Affinity Values Synthesized Up to Date

[125I]PD 164333 [70]	[11C]PD 156707 [52]	[11C]L 753037 [71]
$K_D(ET_A)$ = 0.99 nM $K_D(ET_B)$ = 2.41 μM [70]	$IC_{50}(ET_A)$ = 0.31 nM $IC_{50}(ET_B)$ = 0.42 μM [68,69]	$K_i(ET_A)$ = 0.034 nM $K_i(ET_B)$ = 0.104 nM [72]
[18F]SB 209670 [74]	[123/125I]PD 169390 [76]	[11C]ABT 627 [78]
$K_i(ET_A)$ = 0.41 nM $K_i(ET_B)$ = 199 nM [74,75]	$K_i(ET_A)$ = 0.97 nM $K_i(ET_B)$ = 1.30 μM [76]	$K_i(ET_A)$ = 0.07 nM $K_i(ET_B)$ = 139 nM [77]
[18F]fluorethoxy-PD 156707 [79]	[11C]BMS-5p [80]	[18F]FBz-BMS [80]
$K_i(ET_A)$ = 1.1 nM $K_i(ET_B)$ = 240 nM [79]	$IC_{50}(ET_A)$ = 14.36 nM $IC_{50}(ET_B)$ = n.d. [80]	$IC_{50}(ET_A)$ = 3.09 nM $IC_{50}(ET_B)$ = n.d. [80]

motif. The conjugation of the fluorescent dye active ester (Cy 5.5 NHS-ester) was accomplished by reaction of the two compounds in bicarbonate buffer / DMSO at room temperature. Yields were usually around 70%, determined by HPLC methods. The Cy 5.5-labeled ligand (Fig. **17B**) was used in *in vitro* binding assays of human cancer cells where binding of the photoprobe could be directly analyzed by fluorescence microscopy. Blocking of the signal was possible with an ET$_A$R specific antibody or with unlabeled ligand, confirming target specific binding of the probe. In addition, the biodistribution behaviour of the fluorescent probe was evaluated in wild-type BL6 mice using FRI (Fig. **18**) [86]. Here, a high signal intensity was found in lung, liver and kidney at early time points. While the signal in the kidneys rapidly decreased, signal intensities in lung increased up to 24 hours and the intensity in the liver was nearly constant over this

period of time. The specific *in vivo* binding of the probe was confirmed by predosing experiments, where especially the signal intensity in the heart could be decreased by up to 50%, emphasizing the high ratio of ET$_A$R present in myocardial tissue. An accumulation of the tracer was found in the lung at later time points (24 h – 48 h), where predosing had no effect anymore and a high degree of internalization was proposed.

OUTLOOK

Despite promising preclinical (animal) experiments with radiolabeled or optical tracers and encouraging experiments with human tissue sections an early and straightforward transfer of the described imaging probes to clinical applications is not attainable in the near future. The drawbacks are, indeed, very similar in all molecular imaging approaches.
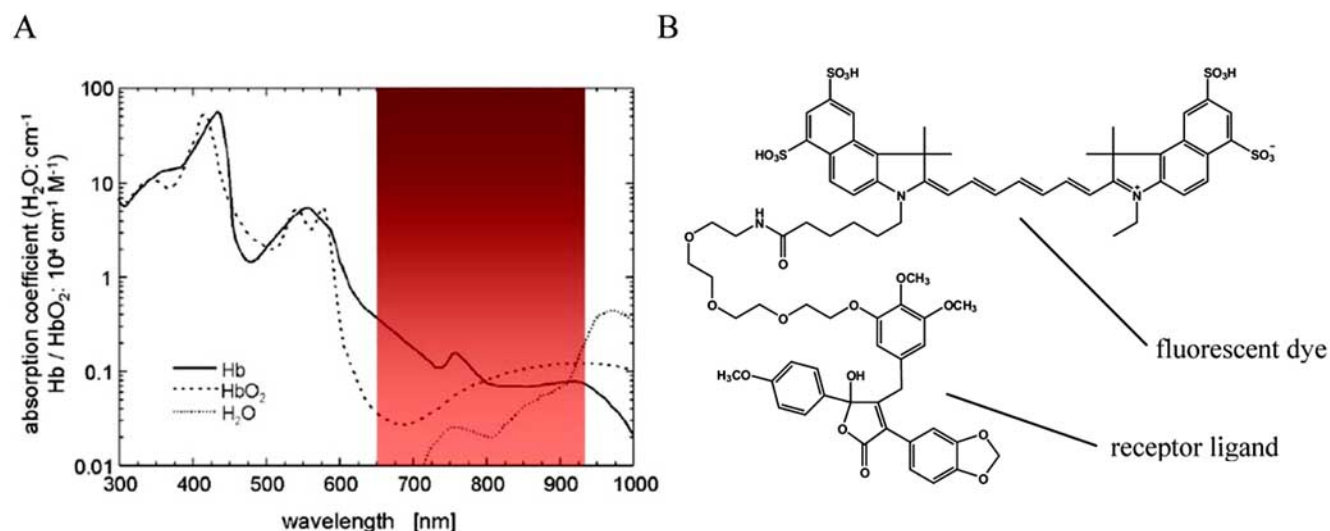
Fig. (17). A) The 'diagnostic window' of near infrared fluorescence (NIRF) imaging. The absorption of hemoglobin (Hb), oxidized hemoglobin (HbO$_2$) and water (H$_2$O) are at a minimum at wavelenghts between 650 nm and 950 nm. B) Structure of the developed endothelin receptor affine fluorescent photoprobe based on PD 156707 [85]. The ligand was modified by assembling of a short polyethylene glycol spacer with an amino residue, which reacted with the active ester of the fluorochrome, yielding a receptor ligand with an amide-bound Cy 5.5 dye.
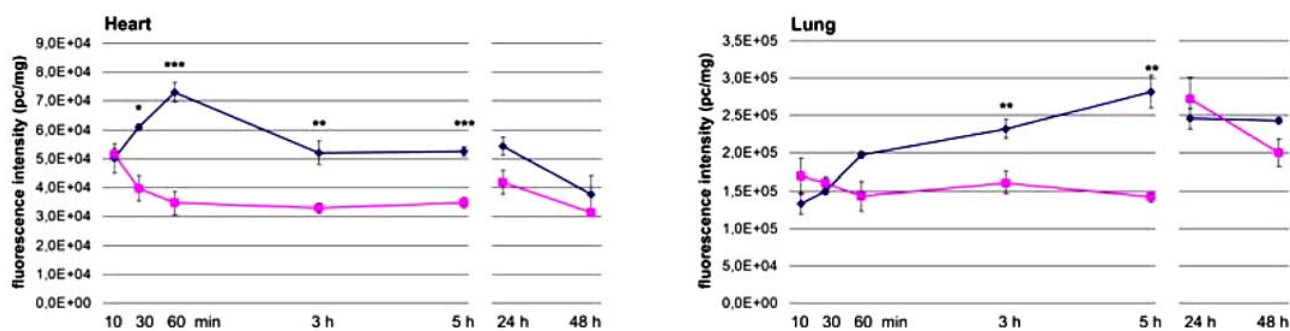

Fig. (18). Fluorescence reflectance imaging (FRI) measurements of murine heart (left) and lung (right) after intraveneous injection of a fluorescent endothelin receptor imaging probe based on PD 156707 with ♦ and without predosing with PD 156707 ■ (wild type CD1 mice, n = 6-8). Signal intensities are expressed as the photon counts per mg of wet tissue weight (pc/mg, mean ± sem). Stars indicate significant differences in intensities (* p ≤ 0.01, ** p ≤ 0.005, *** p ≤ 0.0001, note the difference in scale). Between 30 min and 5 h there is a highly specific signal in heart tissue. Lung values rise constantly values rise constantly from 10 min to 5 h in non predosed animals while predosing led to consistent signal intensity up to 5 h. After one day the tracer has accumulated in lung tissue and predosing had no effect, indicating a high degree of internalization in this organ [86].

The complexity of the biological processes involved in the monitored pathophysiology has still to be elucidated, especially concerning target expression and target processing at different states of the disease. Also, the applicability of preclinical models and their interpretation for a later clinical transfer is controversially discussed. The endothelin axis, however, is a prominent target for further *in vivo* imaging approaches. Its dysregulation is related to a number of severe diseases and a visualization of its nature using state-of-the-art molecular imaging techniques is a great (pre)clinical challenge. For a deeper insight into the subcellular processes affecting the endothelin axis a more elaborate tracer selection and tracer utilization is necessary. The ET$_B$R, for instance, is often discussed as a better target for predicting the progression of cancer cells (e.g. melanoma [30]), because it mediates cell adhesion, migration and invasiveness due to an increase of $\alpha_v\beta_3$- and $\alpha_2\beta_1$-integrin expression and matrix

metalloproteinase (MMP) activation. A selective imaging of ET$_A$R and ET$_B$R in the same experiment, e.g. using different radioactive nuclei, would therefore be very helpful to understand their different influence on certain pathophysiologies.

To develop and synthesize small non-peptidic radioligands for the endothelin receptors, such as those presented in this review, is the most promising approach for a future translation into clinical applications. In this context, the setting up of GCP (good clinical practice)-compliant procedures and the permissions from ethical and public authorities for clinical tests are major obstacles researchers and clinicians have to deal with. Also, as shown in this review, the design of imaging probes by simply attaching a radioisotope to a known ligand molecule is not instantaneously leading to a feasible *in vivo* radiopharmaceutical for use in the clinics. Most often an unfavourable biodistribution or limited stability are the restraining factors. Among these, the lipophilicity,

which usually is expressed by the logP or logD value, represents an important factor that determines the *in vivo* behaviour of (radio)pharmaceuticals. On one hand a high lipophilicity of drugs is necessary to reach specific target organs. For example, for passive penetration of neutral molecules into the central nervous system by crossing the blood brain barrier a logD-value of 2.5-2.7 is suggested [87]. On the other hand Obach *et al.* observed a positive correlation between lipophilicity and plasma protein binding of a drug [88]. Therefore, the distribution of a lipophilic (radio)pharmaceutical is limited due to high plasma protein binding. Additionally, renal clearance decreases with increase in lipophilicity [89]. Consequently, the fine-tuning of tracer lipophilicity is one of the most challenging tasks for the future. This, of course, is applicable for all new tracer compounds, not only for those targeted at the endothelin axis.

The use of optical imaging techniques for *in vitro* imaging approaches is a widespread and customary method. New technologies for *in vivo* molecular imaging applications like FRI and FMT are currently developed to enter clinical practice. It has been shown in numerical simulations as well as in clinical investigations that FMT technology can be scaled up for human use [90]. Besides tomographic imaging modalities, one could also envision a combination of endoscopic or laparoscopic devices with optical fibers for fluorochrome detection. Moreover, handheld scanning devices may be useful tools to screen for superficial fluorochrome detection. Our group has successfully shown, that labeling a small molecular, non-peptidic endothelin receptor ligand with a fluorescent dye is possible and does not impair its binding characteristics. A future use of such modified ligands will enable the evaluation of the endothelin axis *in vivo*.

ACKNOWLEDGEMENTS

REFERENCES

[1]　Blamire, A. M. The technology of MRI - the next 10 years? *Br. J. Radiol.,* **2008**, *81*, 601-617.

[2]　Haberkorn, U. PET and SPECT. *Handb. Exp. Pharmacol.,* **2008**, (185 Pt 2), 13-35.

[3]　Ntziachristos, V.; Bremer, C.; Weissleder, R. Fluorescence imaging with near-infrared light: new technological advances that enable *in vivo* molecular imaging. *Eur. Radiol.,* **2003**, *13*, 195-208.

[4]　Hickey, K. A.; Rubanyi, G.; Paul, R. J.; Highsmith, R. F. Characterization of a coronary vasoconstrictor produced by cultured endothelial cells. *Am. J. Physiol.,* **1985**, *248*, (5 Pt 1), C550-6.

[5]　Yanagisawa, M.; Kurihara, H.; Kimura, S.; Tomobe, Y.; Kobayashi, M.; Mitsui, Y.; Yazaki, Y.; Goto, K.; Masaki, T. A novel potent vasoconstrictor peptide produced by vascular endothelial cells. *Nature,* **1988**, *332*, 411-415.

[6]　Kedzierski, R. M.; Yanagisawa, M. Endothelin system: the double-edged sword in health and disease. *Annu. Rev. Pharmacol. Toxicol.,* **2001**, *41*, 851-876.

[7]　Levin, E. R. Endothelins. *N. Engl. J. Med.* **1995**, *333*, 356-363.

[8]　Masaki, T. Historical review: Endothelin. *Trends. Pharmacol. Sci.,* **2004**, *25*, 219-224.

[9]　Henry, P. J. Endothelin receptor distribution and function in the airways. *Clin. Exp. Pharmacol. Physiol.,* **1999**, *26*, 162-167.

[10]　Cowburn, P. J.; Cleland, J. G. Endothelin antagonists for chronic heart failure: do they have a role? *Eur. Heart J.,* **2001**, *22*, 1772-1784.

[11]　Goldie, R. G. Endothelins in health and disease: an overview. *Clin. Exp. Pharmacol. Physiol.,* **1999**, *26*, 145-148.

[12]　Nelson, J.; Bagnato, A.; Battistini, B.; Nisen, P. The endothelin axis: emerging role in cancer. *Nat. Rev. Cancer,* **2003**, *3*, 110-116.

[13]　Amberg, W.; Hergenroder, S.; Hillen, H.; Jansen, R.; Kettschau, G.; Kling, A.; Klinge, D.; Raschack, M.; Riechers, H.; Unger, L. Discovery and synthesis of (S)-3-[2-(3,4- dimethoxyphenyl)-ethoxy]-2- (4,6-dimethylpyrimidin-2-yloxy)-3,3-diphenylpropionic acid (LU 302872), a novel orally active mixed ET(A)/ET(B) receptor antagonist. *J. Med. Chem.,* **1999**, *42*, 3026-3032.

[14]　Boyd, S. A.; Mantei, R. A.; Tasker, A. S.; Liu, G.; Sorensen, B. K.; Henry, K. J., Jr.; von Geldern, T. W.; Winn, M.; Wu-Wong, J. R.; Chiou, W. J.; Dixon, D. B.; Hutchins, C. W.; Marsh, K. C.; Nguyen, B.; Opgenorth, T. J. Discovery of a series of pyrrolidine-based endothelin receptor antagonists with enhanced ET(A) receptor selectivity. *Bioorg. Med. Chem.,* **1999**, *7* (6), 991-1002.

[15]　Davenport, A. P.; Battistini, B. Classification of endothelin receptors and antagonists in clinical development. *Clin. Sci. (Lond),* **2002**, *103* (Suppl 48), 1S-3S.

[16]　Sakaki, J.; Murata, T.; Yuumoto, Y.; Nakamura, I.; Trueh, T.; Pitterna, T.; Iwasaki, G.; Oda, K.; Yamamura, T.; Hayakawa, K. Discovery of IRL 3461: a novel and potent endothelin antagonist with balanced ETA/ETB affinity. *Bioorg. Med. Chem. Lett.,* **1998**, *8* (16), 2241-2246.

[17]　Webb, M. L.; Meek, T. D. Inhibitors of endothelin. *Med. Res. Rev.,* **1997**, *17* (1), 17-67.

[18]　Bagnato, A.; Natali, P. G. Targeting endothelin axis in cancer. *Cancer Treat. Res.,* **2004**, *119*, 293-314.

[19]　Bagnato, A.; Rosano, L. The endothelin axis in cancer. *Int. J. Biochem. Cell Biol.,* **2008**, *40*, 1443-1451.

[20]　Bagnato, A.; Spinella, F.; Rosano, L. The endothelin axis in cancer: the promise and the challenges of molecularly targeted therapy. *Can J. Physiol. Pharmacol.,* **2008**, *86*, 473-484.

[21]　Dawson, N. A. New molecular targets in advanced prostate cancer. *Expert. Rev. Anticancer Ther.,* **2006**, *6*, 993-1002.

[22]　Fischgräbe, J.; Wülfing, P. Targeted therapies in breast cancer: established drugs and recent developments. *Curr. Clin. Pharmacol.,* **2008**, *3*, 85-98.

[23]　Smollich, M.; Wülfing, P. The endothelin axis: a novel target for pharmacotherapy of female malignancies. *Curr. Vasc. Pharmacol.,* **2007**, *5*, 239-248.

[24]　Bagnato, A.; Spinella, F.; Rosano, L. Emerging role of the endothelin axis in ovarian tumor progression. *Endocr. Relat. Cancer,* **2005**, *12*, 761-772.

[25]　Meidan, R.; Levy, N. The ovarian endothelin network: an evolving story. *Trends. Endocrinol. Metab.,* **2007**, *18*, 379-385.

[26]　Rosano, L.; Spinella, F.; Di Castro, V.; Nicotra, M. R.; Albini, A.; Natali, P. G.; Bagnato, A. Endothelin receptor blockade inhibits molecular effectors of Kaposi's sarcoma cell invasion and tumor growth *in vivo. Am. J. Pathol.,* **2003**, *163*, 753-62.

[27]　Berger, Y.; Bernasconi, C. C.; Juillerat-Jeanneret, L. Targeting the endothelin axis in human melanoma: combination of endothelin receptor antagonism and alkylating agents. *Exp. Biol. Med. (Maywood),* **2006**, *231*, 1111-1119.

[28]　Pelosi, G.; Volante, M.; Papotti, M.; Sonzogni, A.; Masullo, M.; Viale, G. Peptide receptors in neuroendocrine tumors of the lung as potential tools for radionuclide diagnosis and therapy. *Q. J. Nucl. Med. Mol.. Imaging.,* **2006**, *50*, 272-87.

[29]　Sulkowska, M.; Sulkowski, S. Role of endothelins in lung pathology. *Rocz. Akad. Med. Bialymst.,* **1997**, 42 Suppl 1, 101-109.

[30]　Bagnato, A.; Natali, P. G. Endothelin receptors as novel targets in tumor therapy. *J. Transl. Med.,* **2004**, *2*, 16.

[31]　Rubanyi, G. M.; Polokoff, M. A. Endothelins: molecular biology, biochemistry, pharmacology, physiology, and pathophysiology. *Pharmacol. Rev.,* **1994**, *46*, 325-415.

[32]　Elgebaly, M. M.; Kelly, A.; Harris, A. K.; Elewa, H.; Portik-Dobos, V.; Ketsawatsomkron, P.; Marrero, M.; Ergul, A. Impaired insulin-mediated vasorelaxation in a nonobese model of type 2

diabetes: role of endothelin-1. *Can. J. Physiol. Pharmacol.,* **2008**, *86*, 358-364.

[33] Zanatta, C. M.; Gerchman, F.; Burttet, L.; Nabinger, G.; Jacques-Silva, M. C.; Canani, L. H.; Gross, J. L. Endothelin-1 levels and albuminuria in patients with type 2 diabetes mellitus. *Diabetes Res. Clin. Pract.,* **2008**, *80*, 299-304.

[34] Mayes, M. D. Endothelin and endothelin receptor antagonists in systemic rheumatic disease. *Arthritis Rheum.,* **2003**, 48, (5), 1190-1199.

[35] Dhaun, N.; Goddard, J.; Webb, D. J. The endothelin system and its antagonism in chronic kidney disease. *J. Am. Soc. Nephrol.,* **2006**, 17, (4), 943-955.

[36] Sticherling, M. The role of endothelin in connective tissue diseases. *Rheumatology (Oxford)* **2006**, *45* (Suppl 3), iii8-10.

[37] Hirata, Y.; Yoshimi, H.; Takaichi, S.; Yanagisawa, M.; Masaki, T., Binding and receptor down-regulation of a novel vasoconstrictor endothelin in cultured rat vascular smooth muscle cells. *FEBS. Lett.,* **1988**, *239*, 13-17.

[38] Hirata, Y.; Yoshimi, H.; Takata, S.; Watanabe, T. X.; Kumagai, S.; Nakajima, K.; Sakakibara, S. Cellular mechanism of action by a novel vasoconstrictor endothelin in cultured rat vascular smooth muscle cells. *Biochem. Biophys. Res. Commun.,* **1988**, *154,* 868-875.

[39] Ihara, M.; Saeki, T.; Fukuroda, T.; Kimura, S.; Ozaki, S.; Patel, A. C.; Yano, M. A novel radioligand [125I]BQ-3020 selective for endothelin ET(B) receptors. *Life Sci.,* **1992**, *51* (6), PL47-52.

[40] Molenaar, P.; Kuc, R. E.; Davenport, A. P. Characterization of two new ETB selective radioligands, [125I]-BQ3020 and [125I]-[Ala1,3,11,15]ET-1 in human heart. *Br. J. Pharmacol.,* **1992**, *107*, 637-639.

[41] Davenport, A. P.; Kuc, R. E.; Fitzgerald, F.; Maguire, J. J.; Berryman, K.; Doherty, A. M. [125I]-PD151242: a selective radioligand for human ET(A) receptors. *Br. J. Pharmacol.,* **1994**, *111*, 4-6.

[42] Peter, M. G.; Davenport, A. P. Selectivity of [125I]-PD151242 for human, rat and porcine endothelin ET(A) receptors in the heart. *Br. J. Pharmacol.,* **1995**, *114*, 297-302.

[43] Doherty, A. M.; Cody, W. L.; Depue, P. L.; He, J. X.; Waite, L. A.; Leonard, D. M.; Leitz, N. L.; Dudley, D. T.; Rapundalo, S. T.; Hingorani, G. P.; Haleen, S. J.; Ladouceur, D. M.; Hill, K. E.; Flynn, M. A.; Reynolds, E. E. Structure-Activity-Relationships of C-Terminal Endothelin Hexapeptide Antagonists. *J. Med. Chem.,* **1993**, *36*, 2585-2594.

[44] Doherty, A. M.; Cody, W. L.; He, J. X.; Depue, P. L.; Leonard, D. M.; Dunbar, J. B.; Hill, K. E.; Flynn, M. A.; Reynolds, E. E. Design of C-Terminal Peptide Antagonists of Endothelin - Structure-Activity-Relationships of ET-1[16-21,D-His16]. *Bioorg. Med. Chem. Lett.,* **1993**, *3*, 497-502.

[45] Dinkelborg, L. M.; Duda, S. H.; Hanke, H.; Tepe, G.; Hilger, C. S.; Semmler, W. Molecular imaging of atherosclerosis using a technetium-99m-labeled endothelin derivative. *J. Nucl. Med.,* **1998**, *39*, 1819-1822.

[46] Dinkelborg, L.; Hilger, C. S.; Semmler, W.; Speck, U.; Henklein, P. Complexes for use in the Diagnosis of vascular Diseases. EP0772633, 2003.

[47] Johannsen, B.; Jankowsky, R.; Noll, B.; Spies, H.; Reich, T.; Nitsche, H.; Dinkelborg, L. M.; Hilger, C. S. Technetium coordination ability of cysteine-containing peptides: X-ray absorption spectroscopy of a Tc-99 labelled endothelin derivative. *Appl. Radiat. Isotopes,* **1997**, *48*, 1045-1050.

[48] Tepe, G.; Duda, S. H.; Meding, J.; Brehme, U.; Ritter, J.; Hanke, H.; Hilger, C. S.; Claussen, C. D.; Dinkelborg, L. M. Tc-99m-labeled endothelin derivative for imaging of experimentally induced atherosclerosis. *Atherosclerosis,* **2001**, *157*, 383-392.

[49] Gibson, R. E.; Fioravanti, C.; Francis, B.; Burns, H. D. Radioiodinated endothelin-1: a radiotracer for imaging endothelin receptor distribution and occupancy. *Nucl. Med. Biol.,* **1999**, *26*, 193-199.

[50] Walsh, T. F.; Fitch, K. J.; Chakravarty, P. K.; Williams, D. L.; Murphy, K. A.; Nolan, N. A.; Obrien, J. A.; Lis, E. V.; Pettibone, D. J.; Kivlighn, S. D.; Gabel, R. A.; Zingaro, G. J.; Krause, S. M.; Siegl, P. K. S.; Clineschmidt, B. V.; Greenlee, W. J. The Discovery Of L-749,329, A Highly Potent, Orally-Active Antagonist Of Endothelin Receptors. *Abstracts Of Papers Of The American Chemical Society,* **1994**, 208, 145-MEDI.

[51] Bolton, A. E.; Hunter, W. M. The labelling of proteins to high specific radioactivities by conjugation to a 125I-containing acylating agent. *Biochem. J.,* **1973**, *133*, 529-539.

[52] Johnstrøm, P.; Aigbirhio, F. I.; Clark, J. C.; Downey, S. P. M. J.; Pickard, J. D.; Davenport, A. P. Syntheses of the first endothelin-A- and -B-selective radioligands for positron emission tomography. *J. Cardiovasc. Pharmacol.,* **2000**, *36*, S58-S60.

[53] Johnstrøm, P.; Davenport, A. P. *In vitro* characterisation of [F-18]-BQ3020, the first positron emitting ligand synthesised for the endothelin ET(B) receptor. *Br. J. Pharmacol.,* **1999**, *128*, U28-U28.

[54] Jarvis, M. F.; Assal, A. A.; Gessner, G. Pharmacological characterization of the rat cerebellar endothelin ET(B) receptor using the novel agonist radioligand [125I]BQ3020. *Brain Res.,* **1994**, *665*, 33-38.

[55] Johnstrøm, P.; Rudd, J. H.; Richards, H. K.; Fryer, T. D.; Clark, J. C.; Weissberg, P. L.; Pickard, J. D.; Davenport, A. P. Imaging endothelin ET(B) receptors using [18F]- BQ3020: *in vitro* characterization and positron emission tomography (microPET). *Exp. Biol. Med. (Maywood),* **2006**, *231*,736-740.

[56] Johnstrøm, P.; Harris, N. G.; Fryer, T. D.; Barret, O.; Clark, J. C.; Pickard, J. D.; Davenport, A. P. [18F]-Endothelin-1, a positron emission tomography (PET) radioligand for the endothelin receptor system: radiosynthesis and *in vivo* imaging using microPET. *Clin. Sci. (Lond),* **2002**, *103* (Suppl 48), 4S-8S.

[57] Johnstrøm, P.; Fryer, T. D.; Richards, H. K.; Harris, N. G.; Barret, O.; Clark, J. C.; Pickard, J. D.; Davenport, A. P. Positron emission tomography using 18F-labeled endothelin-1 reveals prevention of binding to cardiac receptors owing to tissue-specific clearance by ET(B) receptors *in vivo*. *Br. J. Pharmacol.,* **2005**, *144*, 115-122.

[58] Motte, S.; McEntee, K.; Naeije, R. Endothelin receptor antagonists. *Pharmacol. Ther.,* **2006**, *110*, 386-414.

[59] Breu, V.; Clozel, M.; Burri, K.; Hirth, G.; Neidhart, W.; Ramuz, H. *In vitro* characterisation of Ro 46-8443, the first non-peptide antagonist selective for the endothelin ET(B) receptor. *FEBS. Lett.,* **1996**, *383*, 37-41.

[60] von Geldern, T. W.; Tasker, A. S.; Sorensen, B. K.; Winn, M.; Szczepankiewicz, B. G.; Dixon, D. B.; Chiou, W. J.; Wang, L.; Wessale, J. L.; Adler, A.; Marsh, K. C.; Nguyen, B.; Opgenorth, T. J. Pyrrolidine-3-carboxylic acids as endothelin antagonists. 4. Side chain conformational restriction leads to ET(B) selectivity. *J. Med. Chem.,* **1999**, *42*, 3668-3678.

[61] Barst, R. J.; Rich, S.; Widlitz, A.; Horn, E. M.; McLaughlin, V.; McFarlin, J. Clinical efficacy of sitaxsentan, an endothelin-A receptor antagonist, in patients with pulmonary arterial hypertension: open-label pilot study. *Chest,* **2002**, *121*, 1860-1868.

[62] Fattinger, K.; Funk, C.; Pantze, M.; Weber, C.; Reichen, J.; Stieger, B.; Meier, P. J. The endothelin antagonist bosentan inhibits the canalicular bile salt export pump: a potential mechanism for hepatic adverse reactions. *Clin. Pharmacol. Ther.,* **2001**, *69*, 223-231.

[63] Fouassier, L.; Kinnman, N.; Lefevre, G.; Lasnier, E.; Rey, C.; Poupon, R.; Elferink, R. P.; Housset, C. Contribution of mrp2 in alterations of canalicular bile formation by the endothelin antagonist bosentan. *J. Hepatol.,* **2002**, *37*, 184-191.

[64] Roux, S.; Breu, V.; Ertel, S. I.; Clozel, M. Endothelin antagonism with bosentan: a review of potential applications. *J. Mol. Med.,* **1999**, *77,* 364-376.

[65] Cosenzi, A. Enrasentan, an antagonist of endothelin receptors. *Cardiovasc. Drug Rev.,* **2003**, *21*, 1-16.

[66] Tovar, J. M.; Gums, J. G., Tezosentan in the treatment of acute heart failure. *Ann. Pharmacother.,* **2003**, *37*, 1877-1883.

[67] Murugesan, N.; Gu, Z.; Spergel, S.; Young, M.; Chen, P.; Mathur, A.; Leith, L.; Hermsmeier, M.; Liu, E. C.; Zhang, R.; Bird, E.; Waldron, T.; Marino, A.; Koplowitz, B.; Humphreys, W. G.; Chong, S.; Morrison, R. A.; Webb, M. L.; Moreland, S.; Trippodo, N.; Barrish, J. C. Biphenylsulfonamide endothelin receptor antagonists. 4. Discovery of N-[[2'-[[(4,5-dimethyl-3-isoxazolyl)amino]-sulfonyl]-4-(2-oxazolyl)[1,1'-bi phenyl]- 2- yl]methyl]-N,3,3-trimethylbutanamide (BMS-207940), a highly potent and orally active ET(A) selective antagonist. *J. Med. Chem.,* **2003**, *46*, 125-1137.

[68] Doherty, A. M.; Patt, W. C.; Edmunds, J. J.; Berryman, K. A.; Reisdorph, B. R.; Plummer, M. S.; Shahripour, A.; Lee, C.; Cheng, X. M.; Walker, D. M.; *et al*. Discovery of a novel series of orally active non-peptide endothelin ET(A) receptor-selective antagonists. *J. Med. Chem.,* **1995**, *38*, 1259-1263.

[69]   Doherty, A. M.; Patt, W. C.; Repine, J.; Edmunds, J. J.; Berryman, K. A.; Reisdorph, B. R.; Walker, D. M.; Haleen, S. J.; Keiser, J. A.; Flynn, M. A.; *et al.* Structure-activity relationships of a novel series of orally active nonpeptide ET(A) and ET(A/B) endothelin receptor-selective antagonists. *J. Cardiovasc. Pharmacol.,* **1995**, *26* Suppl 3, S358-61.

[70]   Davenport, A. P.; Kuc, R. E.; Ashby, M. J.; Patt, W. C.; Doherty, A. M. Characterization of [^{125}I]-PD164333, an ET(A) selective non-peptide radiolabeled antagonist, in normal and diseased human tissues. *Br. J. Pharmacol.,* **1998**, *123*, 223-230.

[71]   Ravert, H. T.; Mathews, W. B.; Hamill, T. G.; Burns, H. D.; Dannals, R. F. Radiosynthesis of a potent endothelin receptor antagonist: [^{11}C] L-753,037. *J. Label. Comp. Radiopharm.,* **2000**, *43*, 1205-1210.

[72]   Nishikibe, M.; Ohta, H.; Okada, M.; Ishikawa, K.; Hayama, T.; Fukuroda, T.; Noguchi, K.; Saito, M.; Kanoh, T.; Ozaki, S.; Kamei, T.; Hara, K.; William, D.; Kivlighn, S.; Krause, S.; Gabel, R.; Zingaro, G.; Nolan, N.; O'Brien, J.; Clayton, F.; Lynch, J.; Pettibone, D.; Siegl, P. Pharmacological properties of J-104132 (L-753,037), a potent, orally active, mixed ET(A)/ET(B) endothelin receptor antagonist. *J. Pharmacol. Exp. Ther.,* **1999**, *289*, 1262-1270.

[73]   Aleksic, S.; Szabo, Z.; Scheffel, U.; Ravert, H. T.; Mathews, W. B.; Kerenyi, L.; Rauseo, P. A.; Gibson, R. E.; Burns, H. D.; Dannals, R. F. *In vivo* labeling of endothelin receptors with [^{11}C] L-753,037: studies in mice and a dog. *J. Nucl. Med.,* **2001**, *42*, 1274-1280.

[74]   Johnstrøm, P.; Landvatter, S. W.; Senderoff, S. G.; Clark, J. C.; Pickard, J. D.; Ohlstein, E. H.; Davenport, A. P. Synthesis and preliminary *in vitro* characterisation of a F-18- labeled analogue of SB209670, a PET radioligand for the endothelin receptor. *Br. J. Pharmacol.,* **2001**, 133, 99P.

[75]   Johnstrøm, P.; Fryer, T. D.; Richards, H. K.; Barret, O.; Clark, J. C.; Ohlstein, E. H.; Pickard, J. D.; Davenport, A. P. *In vivo* imaging of cardiovascular endothelin receptors using the novel radiolabelled antagonist [^{18}F]-SB209670 and positron emission tomography (microPET). *J. Cardiovasc. Pharmacol.,* **2004**, *44* (Suppl 1), S34-8.

[76]   Höltke, C.; Law, M. P.; Wagner, S.; Breyholz, H. J.; Kopka, K.; Bremer, C.; Levkau, B.; Schober, O.; Schäfers, M. Synthesis, *in vitro* pharmacology and biodistribution studies of new PD 156707-derived ET(A) receptor radioligands. *Bioorg. Med. Chem.,* **2006**, *14*, 1910-1917.

[77]   Opgenorth, T. J.; Adler, A. L.; Calzadilla, S. V.; Chiou, W. J.; Dayton, B. D.; Dixon, D. B.; Gehrke, L. J.; Hernandez, L.; Magnuson, S. R.; Marsh, K. C.; Novosad, E. I.; Von Geldern, T. W.; Wessale, J. L.; Winn, M.; Wu-Wong, J. R. Pharmacological char-

acterization of A-127722: an orally active and highly potent ET(A) selective receptor antagonist. *J. Pharmacol. Exp. Ther.,* **1996**, *276*, 473-481.

[78]   Mathews, W. B.; Zober, T. G.; Ravert, H. T.; Scheffel, U.; Hilton, J.; Sleep, D.; Dannals, R. F.; Szabo, Z. Synthesis and *in vivo* evaluation of a PET radioligand for imaging the endothelin-A receptor. *Nucl. Med. Biol.,* **2006**, *33*, 15-19.

[79]   Höltke, C.; Wagner, S.; Breyholz, H. J.; Faust, A.; Law, M. P.; Schäfers, M.; Kopka, K. Development, synthesis and *in vitro* evaluation of novel ET(A) receptor PET-radioligands based on PD 156707. *J. Label. Comp. Radiopharm.,* **2007**, *50*, (S1), S345.

[80]   Mathews, W. B.; Murugesan, N.; Xia, J.; Scheffel, U.; Hilton, J.; Ravert, H. T.; Dannals, R. F.; Szabo, Z. Synthesis and *in vivo* evaluation of novel PET radioligands for imaging the endothelin-A receptor. *J. Nucl. Med.,* **2008**, *49*, 1529-1536.

[81]   Bremer, C. Optical methods. *Handb Exp Pharmacol* **2008**, (185 Pt 2), 3-12.

[82]   Bremer, C.; Ntziachristos, V.; Mahmood, U.; Tung, C. H.; Weissleder, R. Progress in optical imaging. *Radiologe,* **2001**, *41*, 131-137.

[83]   Bremer, C.; Ntziachristos, V.; Weissleder, R. Optical-based molecular imaging: contrast agents and potential medical applications. *Eur. Radiol.,* **2003**, *13*, 231-243.

[84]   Ntziachristos, V.; Bremer, C.; Graves, E. E.; Ripoll, J.; Weissleder, R. *In vivo* tomographic imaging of near-infrared fluorescent probes. *Mol. Imaging,* **2002**, *1*, 82-88.

[85]   Höltke, C.; von Wallbrunn, A.; Kopka, K.; Schober, O.; Heindel, W.; Schäfers, M.; Bremer, C. A fluorescent photoprobe for the imaging of endothelin receptors. *Bioconjug. Chem.,* **2007**, *18*, 685-694.

[86]   Höltke, C.; Waldeck, J.; Kopka, K.; Heindel, W.; Schober, O.; Schäfers, M.; Bremer, C. Biodistribution of a non-peptidic fluorescent ET(A) receptor imaging probe. *Mol. Imaging,* **2009**, *8*, 27-34.

[87]   Dishino, D. D.; Welch, M. J.; Kilbourn, M. R.; Raichle, M. E. Relationship between lipophilicity and brain extraction of C-11-labeled radiopharmaceuticals. *J. Nucl. Med.,* **1983**, *24*, 1030-1038.

[88]   Obach, R. S.; Lombardo, F.; Waters, N. J. Trend analysis of a database of intravenous pharmacokinetic parameters in humans for 670 drug compounds. *Drug. Metab. Dispos.,* **2008**, *36*, 1385-1405.

[89]   Varma, M. V.; Feng, B.; Obach, R. S.; Troutman, M. D.; Chupka, J.; Miller, H. R.; El- Kattan, A. Physicochemical Determinants of Human Renal Clearance. *J. Med. Chem.,* **2009**, [Epub ahead of print], DOI: 10.1021/jm900403j.

[90]   Ntziachristos, V.; Ripoll, J.; Weissleder, R. Would near-infrared fluorescence signals propagate through large human organs for clinical studies? *Opt. Lett.,* **2002**, *27*, 333-335.